At the crossroads: strigolactones mediate changes in cytokinin synthesis and signalling in response to nitrogen limitation

Petros P. Sigalas[1,*] (iD), Tom Bennett[2], Peter Buchner[1], Stephen G. Thomas[1], Frank Jamois[3], Mustapha Arkoun[4], Jean-Claude Yvin[4], Malcolm J. Bennett[5] and Malcolm J. Hawkesford[1]

[1]*Rothamsted Research, West Common, Harpenden AL5 2JQ, UK,*
[2]*Faculty of Biological Sciences, School of Biology, University of Leeds, Leeds LS2 9JT, UK,*
[3]*Laboratoire de Physico-Chimie et Bioanalytique, Centre Mondial d'Innovation of Roullier Group, 18 Avenue Franklin Roosevelt, Saint-Malo 35400, France,*
[4]*Plant Nutrition R&D Department, Centre Mondial d'Innovation of Roullier Group, 18 Avenue Franklin Roosevelt, Saint-Malo 35400, France, and*
[5]*Plant and Crop Sciences, School of Biosciences, University of Nottingham, Sutton Bonington Campus, Loughborough LE12 5RD, UK*

SUMMARY

Strigolactones (SLs) are key regulators of shoot growth and responses to environmental stimuli. Numerous studies have indicated that nitrogen (N) limitation induces SL biosynthesis, suggesting that SLs may play a pivotal role in coordinating systemic responses to N availability, but this idea has not been clearly demonstrated. Here, we generated triple knockout mutants in the SL synthesis gene *TaDWARF17* (*TaD17*) in bread wheat and investigated their phenotypic and transcriptional responses under N limitation, aiming to elucidate the role of SLs in the adaptation to N limitation. *Tad17* mutants display typical SL mutant phenotypes, and fail to adapt their shoot growth appropriately to N. Despite exhibiting an increased tillering phenotype, *Tad17* mutants continued to respond to N limitation by reducing tiller number, suggesting that SLs are not the sole regulators of tillering in response to N availability. RNA-seq analysis of basal nodes revealed that the loss of D17 significantly altered the transcriptional response of N-responsive genes, including changes in the expression profiles of key N response master regulators. Crucially, our findings suggest that SLs are required for the transcriptional downregulation of cytokinin (CK) synthesis and signalling in response to N limitation. Collectively, our results suggest that SLs are essential for the appropriate morphological and transcriptional adaptation to N limitation in wheat, and that the repressive effect of SLs on shoot growth is partly mediated by their repression of CK synthesis.

Keywords: strigolactones, cytokinin, nitrogen, RNA-seq, wheat, *Triticum aestivum*, tillering.

INTRODUCTION

Since their discovery as plant hormones and pivotal regulators of axillary branching (in grasses, known as tillering), strigolactones (SLs) have attracted significant research interest. Studies across various species, particularly in Arabidopsis (*Arabidopsis thaliana*) and rice (*Oryza sativa*), have advanced our understanding of the SL biosynthetic and signalling pathways, unravelling the involvement of SLs in diverse developmental processes and plant responses to environmental cues (Chesterfield et al., 2020). The core SL biosynthetic pathway, conserved across species, comprises a β-carotene isomerase known as

DWARF27 (D27), along with two carotenoid cleavage dioxygenases (CCD), CCD7 and CCD8 (in grasses, typically called DWARF17 and DWARF10 respectively), which catalyse the three-step conversion of β-carotene into carlactone. The biosynthetic pathway downstream of carlactone exhibits extensive variation among species and likely contributes to the structural diversity observed in naturally occurring SLs (Clark & Bennett, 2024; Yoneyama & Brewer, 2021). However, most downstream pathways involve the activity of members of the cytochrome P450 CYP711A subfamily, also known as MORE AXILLARY BRANCHING1 (MAX1), which have been identified as

crucial enzymes in the conversion of carlactone to bioactive SLs, as evidenced in numerous studies across different species (Abe et al., 2014; Marzec et al., 2020; Wu & Li, 2021; Yoneyama et al., 2018; Zhang et al., 2014). Three key classes of protein are involved in SL signalling; a/b-hydrolases of the DWARF14 (D14) family which act as SL receptors; members of the SMXL7/DWARF53 (D53) family that are the proteolytic targets of SL signalling and transcriptional repressors of SL signalling pathway downstream genes, and MAX2/D3 F-box proteins which mediate the interaction between D14 and D53 as part of an SCF-type ubiquitin ligase complex (Machin et al., 2020). Upon SL binding, D14 undergoes conformational changes that allow interaction with D3 and D53, and result in the ubiquitination and degradation of D53, allowing downstream transcription responses to occur (Seto, 2024; Waters et al., 2017).

Numerous studies have shown that SL biosynthesis is induced by nutrient limitations, such as phosphorus (P) and nitrogen (N) (Kohlen et al., 2011; Umehara et al., 2008, 2010; Yoneyama et al., 2012, 2015; Yoneyama, Xie, et al., 2007; Yoneyama, Yoneyama, et al., 2007). N is an essential macronutrient for plants as it is a fundamental component of DNA, amino acids, proteins, chlorophyll, hormones, and cell structural components (Ueda et al., 2017). Consequently, N nutrition has a substantial impact on plant metabolism, growth, and productivity. Plant adaptation to N limitation includes a myriad of morphological, physiological, and transcriptional changes that allow plants to optimise their growth based on the available resources. In wheat, several studies have revealed the profound influence of N status on genes related to N uptake and assimilation, nutrient remobilisation, as well as pathways such as central metabolism and photosynthesis, highlighting the pleiotropic effects of N limitation on plant metabolism and growth (Meng et al., 2021; Wang et al., 2019). Studies in Arabidopsis and rice, using systems biology approaches, have elucidated transcription factors (TFs) functioning as master regulators of N-responsiveness upon exposure to nitrate or under N-limiting conditions (Gaudinier et al., 2018; Ueda et al., 2020). These studies have provided valuable insights into the regulation of N-responsive genes but also emphasised the complexity of the N response. Although changes that govern root architectural changes in response to N limitation are well studied, there is a gap in understanding above-ground morphological adaptations such as regulation of tillering, particularly in crop species like bread wheat.

The response to nutrient-limiting conditions requires not only sensing mechanisms in the roots but also local and systemic signals to coordinate the growth of roots and shoots at the whole-plant level. Plant hormones are likely candidates for orchestrating the systemic response to N status to modulate axillary bud outgrowth. Indeed, the synthesis of cytokinin (CK) has long been linked to soil N status, and they are considered long-distance signals of N status (Sakakibara, 2021; Sakakibara et al., 2006). Furthermore, N availability has also been shown to trigger changes in SL biosynthesis in rice (Sun et al., 2014, 2021; Xu et al., 2015). Recently, it was shown that N limitation leads to a systemic induction of SL biosynthetic genes in wheat (Sigalas et al., 2023).

As the major determinant of shoot system size and complexity, axillary branching is a tightly regulated process, particularly with respect to nutritional status and environmental conditions (Walker & Bennett, 2018). Axillary branching consists of two distinct steps: first, the initiation of axillary meristems in the axil of each leaf to form an axillary 'bud', and second the outgrowth of the bud to form a branch (Kebrom et al., 2013). Meristem initiation is generally unaffected by environmental conditions, while outgrowth is strongly environmentally sensitive. For instance, in response to N limitation in rice, bud outgrowth is strongly downregulated, but meristem initiation is unaffected (Luo et al., 2017). The outgrowth of axillary buds is known to be controlled by systemic signals including the plant hormones auxin, SL, and CK, while sugar/energy signalling and light quality perception in each bud have also been shown to play important roles in controlling bud outgrowth (Barbier et al., 2019). Studies in various species have identified members of the *TEOSINTE BRANCHED1* (*TB1*) class of TCP TFs, such as BRANCHED1 (BRC1) in Arabidopsis (Aguilar-Martínez et al., 2007) and FINE CULM1 (FC1) in rice (Minakuchi et al., 2010), as local regulators of axillary bud outgrowth (reviewed in Walker & Bennett, 2018). In Arabidopsis and pea (*Pisum sativum*), the various systemic and environmental signals regulating bud outgrowth converge on *BRC1* transcription, and if BRC1 transcription becomes sufficiently low, bud outgrowth is promoted (Dun et al., 2012; Seale et al., 2017), via a conserved transcriptional response in buds (van Es et al., 2024).

While the role of SLs has been extensively studied in rice, their functional role remains relatively underexplored in other grass crop species, such as bread wheat (*Triticum aestivum*). Recently, Zhao et al. (2020) demonstrated that manipulation of *TaD27* expression, which encodes the enzyme D27 involved in the first step of SL core biosynthetic pathway, leads to altered tiller number in wheat. Specifically, *TaD27-RNAi* lines and *TaD27* overexpressing lines exhibited increased and decreased tiller numbers, respectively, thereby confirming the pivotal role of SLs in regulating tillering in wheat (Zhao et al., 2020). Interestingly, transcriptomic analysis of SL-related genes in response to N limitation in wheat suggests that SL might be much more prominent in N-responsive regulation of shoot growth than previously thought (Sigalas et al., 2023). While SLs are involved in the response to N limitation in

Arabidopsis, they are much more prominent in the response to P limitation (De Jong et al., 2014; Kohlen et al., 2011). However, in wheat, SL synthesis was much more strongly induced by N limitation than P limitation (Sigalas et al., 2023). Following on from these observations, the objectives of this study were first to investigate the role of SLs in wheat tillering regulation in response to N limitation, and second to identify how they regulate systemic plant growth responses to N limitation.

RESULTS

Loss of *D17* in wheat is associated with increased tillering and changes in resource allocation

To test the role of SLs in N limitation in wheat, we attempted to create mutants in TaD17, an important enzyme of the core SL biosynthetic pathway. Triple knock-out *Tad17* mutants were generated by using mutant lines from the hexaploid wheat TILLING population and validated by sequencing. Three nonsense mutant alleles, one per *TaD17* homoeologue, were stacked by crossing (as described in "Experimental Procedures" section). The predicted truncated proteins are lacking important amino acid residues for the functionality of CCD7/D17, suggesting the loss of function of the encoded proteins in these lines (Figure S1). As expected from previous work, the resulting *Tad17* mutants showed an increased tillering phenotype compared with WT, leading to a higher number of spikes per plant, and overall reduced height (Figure 1A; Figure S5a,b).

To test the role of SLs in the response to N limitation, *Tad17* mutants were grown hydroponically supplied with 10 mm of N (High N) or subjected to N stress by providing 0.1 mm of N for 12 days (Low N). Consistent with the previous observation, *Tad17* mutants formed more tillers than WT under both N regimes (Figure 1B,C). Interestingly, *Tad17* showed a proportional reduction in tiller outgrowth when grown under low N conditions that were comparable to the WT (32% reduction in WT and 27% in *Tad17*). ANOVA revealed no significant two-way interaction, which supports the absence of a genotype-specific response to N limitation ($F[1,18] = 0.3$, $P = 0.589$). Apart from changes in tillering, *Tad17* mutants showed reduced root biomass accumulation compared with WT, which was more profound under N-limiting conditions, whereas WT showed no decrease (Figure 1D). Shoot biomass in *Tad17* mutants was lower than WT only under N limitation, although both genotypes showed reduced shoot root biomass in low N (Figure 1E). Plant response to N-limiting conditions involves changes in resource allocation for root and shoot growth, as plants prioritise root growth over shoot growth, which is reflected by an increase in root/shoot ratio (Figure 1F). Although *Tad17* showed an increase in root/-shoot ratio when grown under low N, root/shoot was

significantly lower under N-limiting conditions compared with WT control, suggesting an effect of SLs on N limitation response.

Readings using the Soil Plant Analysis Development (SPAD) chlorophyll meter were taken from different leaves of both genotypes, serving as a proxy of leaf N status (Figure 1G). Plant response to N-limiting conditions involves remobilisation of N from older tissue to developing tissues to support growth, resulting in lower SPAD values. All examined leaves of plants grown under N-limiting conditions showed a significant decrease in SPAD values, but the *TaD17* mutants had an effect on SPAD dynamics in response to N limitation. *Tad17* mutants showed a less strong decrease in SPAD reading in the first and second leaves in response to N limitation compared with WT, but the third leaf showed the same SPAD response as WT. Overall, these results support the idea that SLs play a role in the systemic coordination of growth responses to N limitation.

Transcriptional changes in basal nodes of *Tad17* revealed greater changes under N-limiting conditions

To better understand the involvement of SLs in tillering and on N limitation response, total RNA was extracted from basal nodes of 18-day-old plants grown under high and low N supply for 8 days and submitted for RNA-seq. On average, 39.5 million paired-end reads were acquired per sample, with 85% mapped to the wheat reference genome and 72% uniquely mapped. On average, 57% (53.9–61.8%) of the reads were finally assigned to genes; that is, on average, 26.3 M reads were assigned to genes per sample. More specifically, 62% of the HC genes (67 255 HC) and 15% of the LC genes (24 096 LC) passed the prefiltering and were included in the analysis. For transcript abundance calculation, the Kallisto tool was utilised, resulting in 76% of reads pseudo-aligning to the wheat reference genome. RNA-seq statistics can be found in Table S6, while gene transcript abundances are in Data S1.

Principal component analysis showed the presence of four clusters corresponding to different genotypes and N treatment combinations, suggesting good biological and sequencing repeatability (Figure S6a,b). Samples within the same genotypes but from different BC$_1$F$_3$ populations also clustered together suggesting that the observed transcriptomic changes are less likely to be due to the background mutation load of the mutant lines. N limitation had a substantial effect in the transcriptome of both genotypes and was the main source of differential expression (Figure S6a). In total, 14 741 genes were differential expressed in response to N limitation in WT plants, with N limitation leading to the downregulation of 6832 genes and upregulation of 7909 (Figure S6c; Table S7). In *Tad17*, 13 013 genes were found to be differentially expressed between the two N regimes (Figure S6d; Table S8).
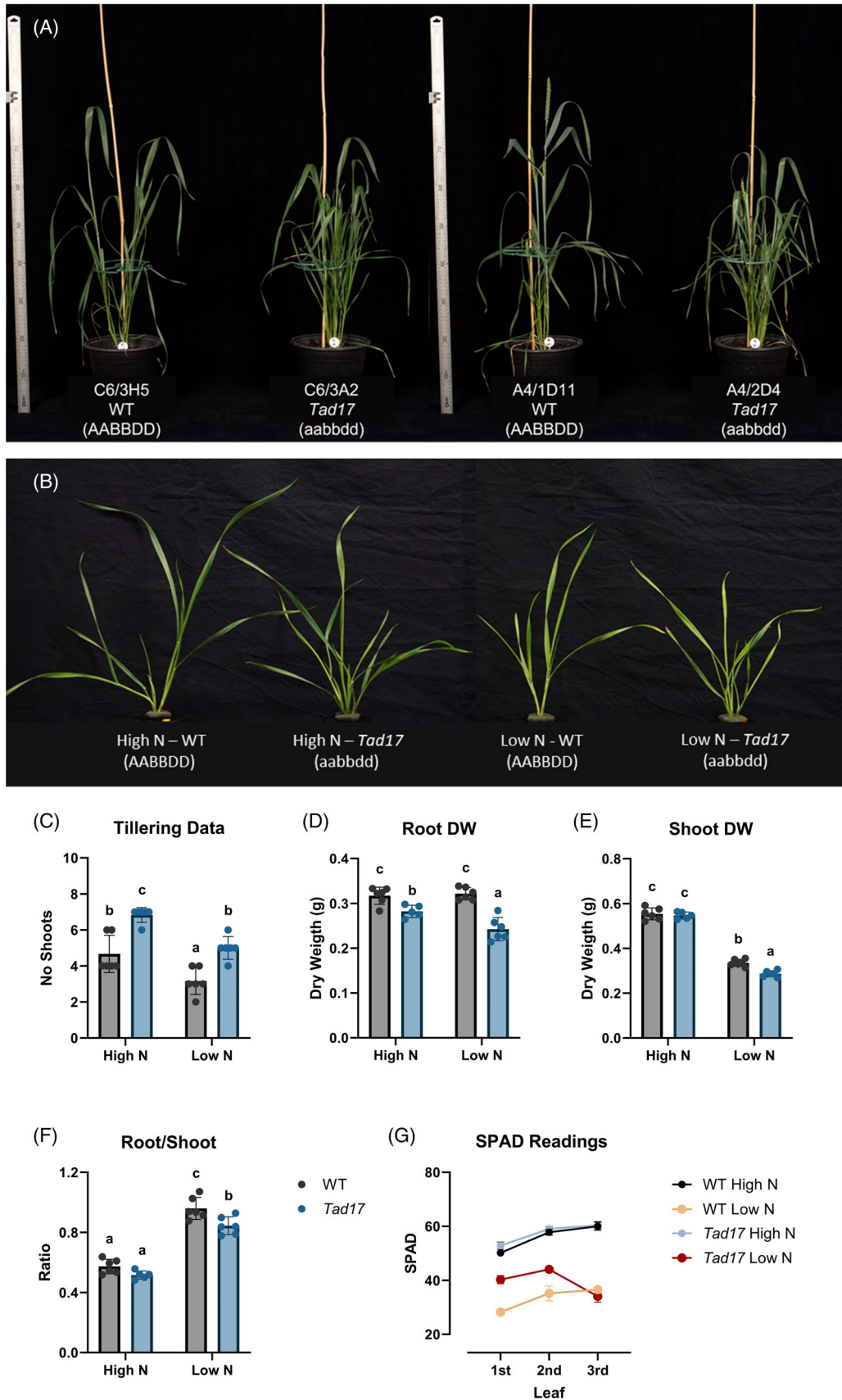
Figure 1. Phenotypic differences and responses of *Tad17* (aabbdd) mutant plants compared with wild-type (WT) (AABBDD) plants under varying N conditions.
(A) Phenotypic comparison of *Tad17* mutant lines from two distinct BC$_1$F$_2$ populations alongside their corresponding WT sibling lines at ear emergence stage.
(B) Representative plants illustrating phenotypic response, (C) number of shoots, (D) root dry weight (DW), (E) shoot DW, and (F) root/shoot ratio of 3-week-old hydroponically cultivated *Tad17* and WT segregant lines grown under high N conditions or subjected to N limitation for 12 days. Each bar corresponds to the mean value of six biological replicates, with error bars indicating the standard error. Individual data points are also depicted as dots on the corresponding bars. Different letters denote statistically significant differences (two-way ANOVA followed by Tukey's Honest Significant Difference test, $P = 0.05$).
(G) Average Soil Plant Analysis Development (SPAD) readings across the first, second, and third leaf of each genotype under high N and low N conditions. Repeated measures ANOVA was used for statistical analysis.

Under high N conditions, 1320 genes exhibited significant differential expression between the WT and *Tad17* mutants (Figure 2A; Table S9). Specifically, 768 genes were downregulated (653 HC and 115 LC), while 552 genes were upregulated (467 HC and 85 LC) in *Tad17*. However, the effect of *TaD17* knock-out was notably stronger under N-limiting conditions (Figure 2B; Table S10). In fact, under N-limiting conditions the number of differentially expressed genes (DEGs) between the two genotypes was four times higher than under high N conditions. In total, 5835 genes were significantly differentially expressed under N-limiting conditions in *Tad17* compared with WT segregant. Knock-out of *TaD17* resulted in significant downregulation of 3389 genes (2870 HC and 519 LC) and upregulation of 2446 genes (2061 HC and 385 LC) in the basal nodes. In total, 1398 genes showed a significant two-way interaction between factors genotype and N level based on the linear model fitted in DESeq2 (Table S11).

Functional annotation enrichment analysis of *Tad17* DEGs

For the biological interpretation of the transcriptional changes in *Tad17* nodes Gene Ontology (GO) and KEGG enrichment analysis were carried out. The analysis revealed a greater number of enriched terms in the DEGs between *Tad17* and WT under N-limiting conditions compared with high N supply (Figure 2C–F; Tables S12–S15). This was anticipated as the effect of *TaD17* knock-out resulted in more substantial transcriptional changes under N-limiting conditions, suggesting a broader impact of SLs on regulation of various biological processes under low N. Many of the enriched GO and KEGG terms were common in both comparisons, indicating that there are some shared biological processes and pathways controlled by SLs regardless of the plant N status (Figure 2C–F).

Unsurprisingly, the terms 'strigolactone metabolic process' (GO:1901600) and 'strigolactone biosynthetic process' (GO:1901601) and KEGG term 'carotenoid biosynthesis' were among the top enriched terms in both N conditions indicating changes in gene expression levels of SL metabolic genes in *Tad17* (Figure 2C–F; Tables S12–S15). 'Secondary shoot formation' (GO:0010223) was also enriched, indicating changes in genes related to tillering regulation which was consistent with the observed phenotypic differences in tiller number in *Tad17*.

More surprisingly, terms related to photosynthesis such as 'photosynthesis light-harvesting' (GO:0009765),

'photosynthesis' (GO:0015979), 'chlorophyll-binding' (GO:0016168), and others were consistently enriched in *Tad17* under both N conditions (Figure 2C,E). Further examination revealed that the same terms were exclusively enriched in the list of downregulated genes suggesting a systematically lower transcript abundance of photosynthesis-related genes in *Tad17* (Tables S13 and S14). The presence of many enriched terms related to carbohydrate metabolism and transport, such as 'disaccharide biosynthetic process' (GO:0046351), 'carbohydrate biosynthetic process' (GO:0016051), 'carbohydrate metabolic process' (GO:0005975) and 'carbohydrate transport' (GO:0008643) also suggests a potential link between SLs and carbohydrate signalling pathways. In fact, the GO term 'trehalose metabolic processes' (GO:0005991) was also found enriched in the list of DEGs between *Tad17* and WT independent of the N supply. Trehalose 6-phosphate (Tre6P) is known to act as a signal of the sugar status affecting developmental decision making, including bud outgrowth (Fichtner et al., 2017, 2021; Figueroa et al., 2016).

Exclusive enrichment of GO terms in *Tad17* under low N conditions suggests interactions between SLs and other hormonal pathways, indicating that SLs interact with other hormonal pathways predominately when N is a limiting factor. In fact, the 'cytokinin metabolic process' (GO:0009690), 'gibberellin metabolic process' (GO:0009685) and 'indole-containing compound metabolic process' (GO:0042430) were enriched only under N-limiting conditions (Figure 2E; Table S13). In addition, the GO: MF term 'cytokinin dehydrogenase activity' (GO:0019139) was also found to be overrepresented, further supporting a link between CK and SLs (Table S13). Consistently, KEGG term 'zeatin biosynthesis' was also significantly enriched in the list of DE in *Tad17* under N-limiting conditions (Figure 2F), and particularly among the upregulated genes (Table S15).

KEGG enrichment analysis also revealed that amino acid metabolism was affected in *Tad17*. More specifically, 'alanine aspartate and glutamate metabolism', 'metabolism of other amino acids', and 'cyanoamino acid metabolism' were significantly enriched in both high N and low N *Tad17* compared with the respective WT control (Figure 2D,F; Tables S14 and S15). In addition, under low N conditions, terms such as 'arginine and proline metabolism' and 'phenylalanine tyrosine and tryptophan biosynthesis' were also found to be enriched, suggesting that *Tad17* showed altered expression of genes involved in a
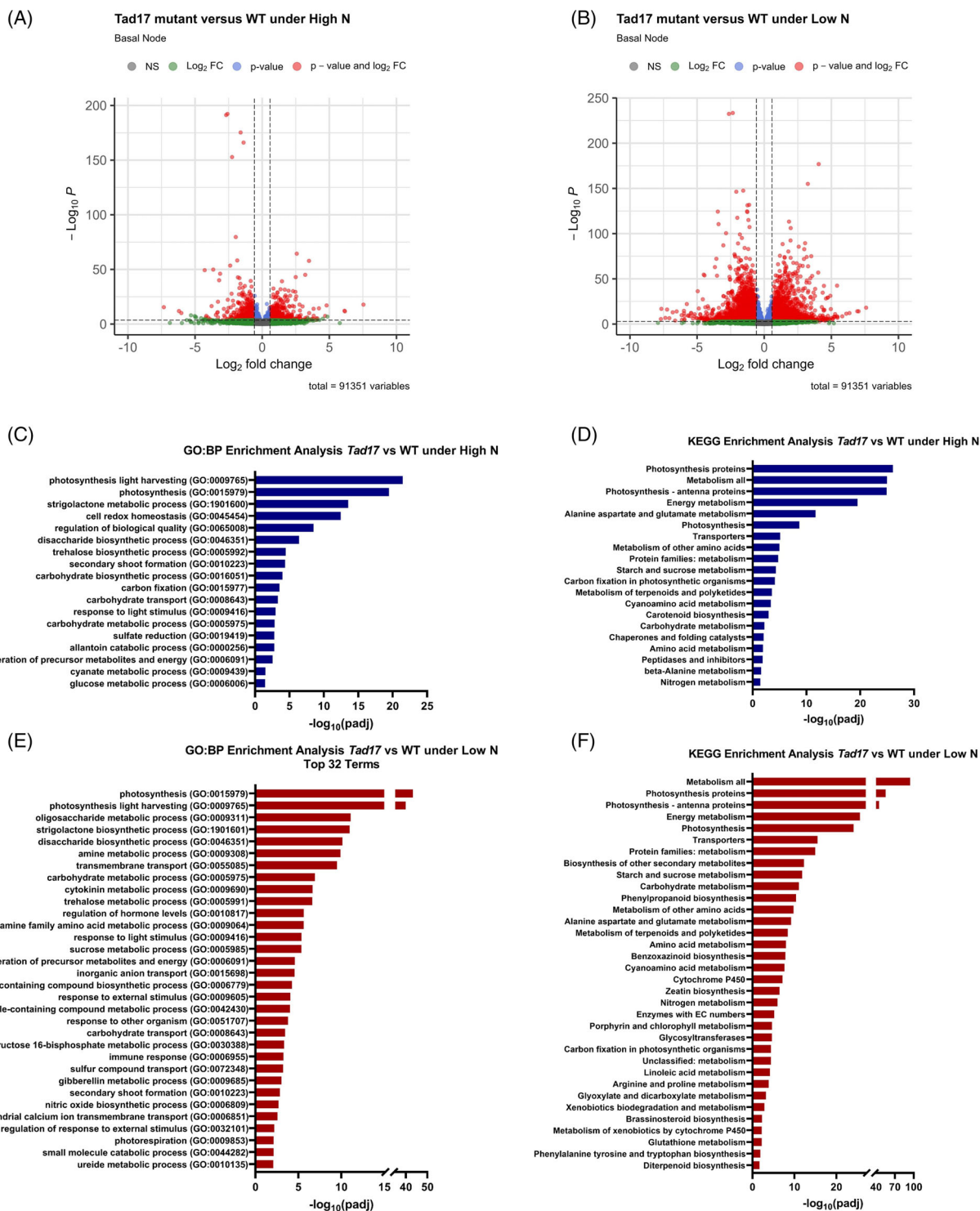
Figure 2. Transcriptional changes in *Tad17* compared with WT segregant under high N and low N conditions.
(A) Volcano plot of the differential gene expression analysis under high N and (B) under low N conditions.
(C) Enriched GO: BP and (D) KEGG terms in the differentially expressed genes in *Tad17* under high N.
(E) Top 32 enriched GO: BP and (F) KEGG terms in the differentially expressed genes in *Tad17* under low N conditions.

wider range of amino acid metabolism under N-limiting conditions.

SL synthesis and signalling genes show feedback regulation in *Tad17*

Strigolactone metabolic pathway was one of the main pathways affected in *Tad17*, evidenced by significant changes in transcript abundance of numerous SL biosynthesis and signalling genes in *Tad17*. The heatmap in Figure 3(A) illustrates the transcriptional responses of all expressed (transcripts per million [TPM] >0.5) SL-related genes in the basal nodes. Notably, *TaD27* and *TaD10* exhibited significant upregulation in *Tad17* nodes under both N conditions compared with the respective WT control. Analysis of *TaMAX1* homoeologues showed that some of the CYP711A encoding clades were also induced in the *Tad17* mutant but to a lesser extent. Consistent with findings in other species, our results suggest a negative feedback mechanism regulating SL biosynthetic genes in wheat nodes, as observed in studies on rice and Arabidopsis SL-deficient or -insensitive mutants (Mashiguchi et al., 2009; Umehara et al., 2008; Waters et al., 2012).

In addition to known wheat SL biosynthetic genes, an orthology search revealed that TraesCS3A02G255100, TraesCS3B02G287100, and TraesCS3D02G256000 are orthologous to Arabidopsis SABATH methyltransferase (AT4G36470) involved in methyl-carlactonate (Me-CLA) biosynthesis downstream of MAX1 (Wakabayashi et al., 2021) and all three homoeologues were strongly induced in basal nodes of *Tad17*, showing a similar pattern to other SL biosynthetic genes. Furthermore, TraesCS3A02G457700, TraesCS3B02G497900, and TraesCS3D02G450500 are orthologues of *AtLBO1* (AT3G21420), which catalyse the conversion of Me-CLA to 1′-OH-Me-CLA, a biologically active non-canonical SL (Brewer et al., 2016) and all three homoeologues were induced in basal nodes of *Tad17*. Thus, based on orthology and strong transcriptional responses in *Tad17*, similar to other SL biosynthetic genes, these genes are likely involved in SL biosynthesis in wheat nodes.

In addition, *Tad17* showed changes in SL perception and signalling genes (Figure 3A). *TaD14* homoeologues were downregulated in *Tad17* compared with WT in both conditions. *TaD3* was not significantly differentially expressed in *Tad17* relative to WT but shows the same
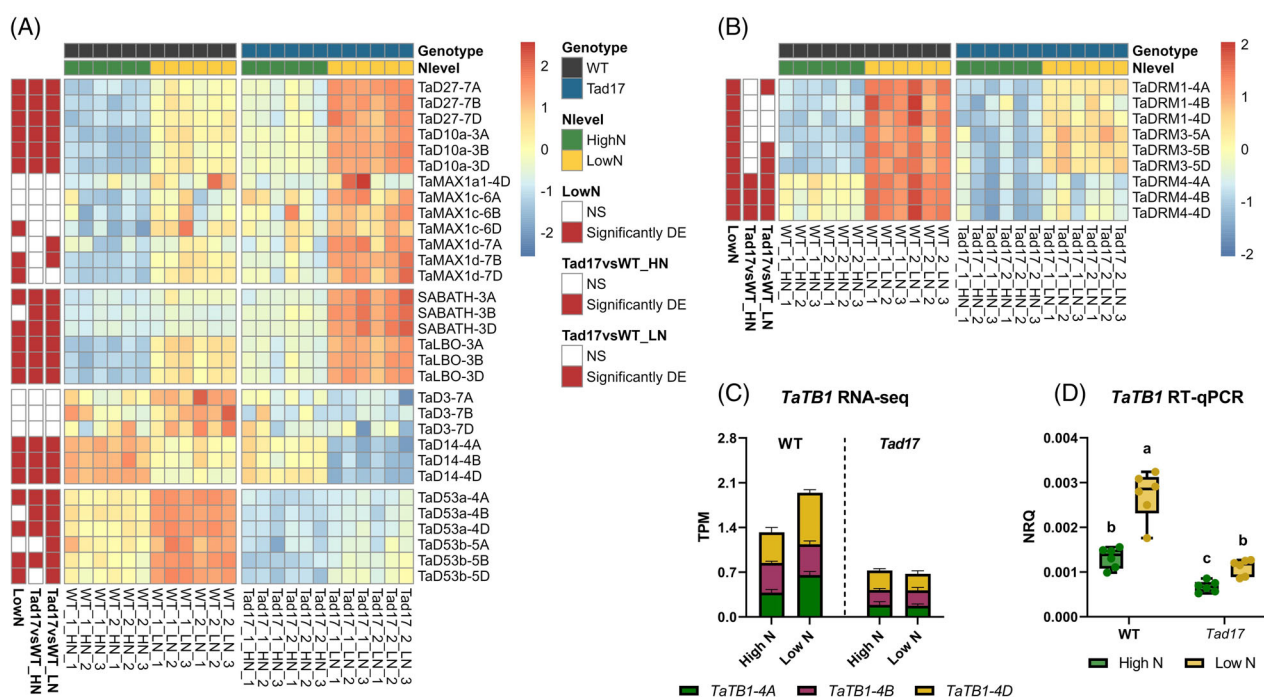
Figure 3. Transcriptional regulation of (A) strigolactone (SL) biosynthesis, perception and signalling, (B) *DRM* and (C, D) *TB1* genes in the basal node of *Tad17* mutant and WT segregant grown under high N (10 mM) or low N (0.1 mM) conditions for 8 days.

(A, B) Each row corresponds to a different gene, while columns correspond to different samples grouped by treatment. Data are *Z*-scores of regularised log normalised counts (rlog) as generated by DESeq2. Warm colours correspond to higher transcript levels, while cold colours to lower levels. Row names correspond to the gene name. Row annotations indicate significant differential gene expression in N-limited nodes, in *Tad17* mutant under high N and in *Tad17* under low N conditions (from left to right).

(C) Transcript abundance of *TaTB1* homoeologues based on RNA-seq. Values are means of six biological replicates and error bars represent standard error.

(D) Expression analysis of *TaTB1* by quantitative reverse-transcription PCR. Different letters denote statistically significant differences between group means (two-way ANOVA followed by Tukey's Honest Significant Difference test, *P* = 0.05).

general pattern of changes. Furthermore, transcript abundance of *TaD53a and TaD53b* homoeologues, which act as transcriptional repressors controlling the transcription of downstream genes and their own transcription forming a negative feedback loop (Jiang et al., 2013; Soundappan et al., 2015; Wang et al., 2015), was significantly reduced in *Tad17* nodes compared with WT, suggesting significant downregulation of the SL signalling pathway.

Response of *DRM* and *TB1* in basal nodes of *Tad17*

DORMANCY-ASSOCIATED PROTEIN-LIKE (DRM) encoding genes serve as molecular markers of bud dormancy in various species (Tarancón et al., 2017). A significant induction of all three homoeologues of *TaDRM1*, *3*, and *4* by N limitation was recorded based on the RNA-seq results, suggesting that N availability controls tillering by influencing bud dormancy (Figure 3B). *TaDRM4* homoeologues were significantly downregulated in basal nodes of *Tad17* mutants under both N conditions, suggesting an influence of SLs on DRM regulation. Notably, among the nine wheat DRM genes identified, the three homoeologues of *TaDRM4* exhibited the highest transcript abundance. Under N-limiting conditions, two homoeologues of *TaDRM3* and *TaDRM1-4A* were also downregulated in *Tad17* mutants (Figure 3B). However, DRM genes were induced by N limitation even in *Tad17*, yet to a lesser extent, indicating that SLs are not the sole signal controlling DRM expression in response to plant N status. This aligns with the observed phenotypic response, as *Tad17* plants showed a reduction in tiller number when grown under low N conditions.

In grasses, the expression of *TB1* genes, homologues of Arabidopsis *BRC1*, are known to be associated with the regulation of tillering across species. *BRC1* is considered a downstream target of the SL signalling pathway in Arabidopsis, but this may not be the case for *TB1* in grasses (Bennett & Leyser, 2014). *TaTB1* homologues were insufficiently expressed in basal nodes to be analysed by RNA-seq (Figure 3C), therefore, to investigate its transcriptional regulation in *Tad17* mutants, expression was also analysed using quantitative reverse-transcription PCR (RT-qPCR) (Figure 3D; Table S16). Our results demonstrated a downregulation of *TaTB1* expression in *Tad17* mutants, particularly under N-limiting conditions. *TaTB1* transcript abundance was significantly induced by N limitation in WT segregant, yet a weaker induction was observed in *Tad17* mutant. The attenuated induction of *TaTB1* expression in *Tad17* mutants under N limitation indicates that while SLs play a significant role in mediating *TB1* upregulation to repress tillering in wheat, other pathways may also contribute to this regulation.

### *Tad17* showed significant changes in N-responsive genes

As mentioned above, transcriptional analysis revealed significant changes in gene expression patterns in response to N limitation. Specifically, we observed the downregulation of 6832 genes and the upregulation of 7909 genes in the basal nodes, referred to as N-responsive genes. The transcriptional response to N limitation led to changes in genes associated with central metabolism, mRNA translation, protein synthesis, N metabolism, as well as various hormonal pathways and TFs. These transcriptional changes are likely to be associated with the general plant adaptation to N-limiting environments.

The expression of 2577 N-responsive genes was significantly different in N-limited basal nodes of *Tad17* mutant compared with WT control, indicating the potential involvement of SLs in the transcriptional regulation of the response to N. Further analysis revealed that these genes could be categorised into four distinct clusters based on their response to N limitation and the response observed in *Tad17* plants (Figure 4A; Table S17). Genes of clusters 1 and 2 were further clustered into sub-clusters based on their overall expression pattern as shown in Figure S7, but for simplicity, only cluster information will be discussed. More specifically, cluster 1 comprised 1098 N-inducible genes, whose transcript abundance was notably lower in the nodes of *Tad17* compared with the WT under N-limiting conditions. This suggests that SLs may be required for the transcriptional response of those genes to N limitation, or at least the lack of SLs decreases the rate of induction by N limitation. On the other hand, cluster 2 contained 610 genes that were suppressed by N limitation, yet their transcript abundance was higher in the N-limited nodes of *Tad17*. Cluster 3 contained 484 genes whose expression was induced by N limitation, but the induction was more pronounced in *Tad17* mutants. Finally, cluster 4 included 385 genes repressed by N, which exhibited significantly lower expression levels in the *Tad17* mutant.

Plant response to N deficiency involves changes in N metabolic genes, nitrate transporters, and amino acid metabolism. Changes in amino acid metabolism facilitate N reassimilation, while changes in amino acid and nitrate transport contribute to N remobilisation and partitioning among different tissues, an important part of plant adaptation to N-limiting conditions. KEGG terms 'nitrogen metabolism', 'amino acid metabolism', and GO: BP terms 'glutamine family amino acid metabolic process' (GO:0009064), 'inorganic anion transport' (GO:0015698), 'amino acid transport' (GO:0006865) and 'nitrate assimilation' (GO:0042128) were enriched among the N-responsive genes affected in N-limited *Tad17* (Figure 4B,C; Tables S18 and S19). These observations suggest a requirement for SLs in coordinating N metabolism and remobilisation under N-limiting conditions. More specifically, terms related to nitrate metabolism were enriched among genes within cluster 2, indicating that the SL-deficient mutant showed reduced downregulation of nitrogen metabolism in response to N deficiency (Tables S20 and S21). On the contrary, the 'ureide catabolic process' (GO:0010136) was
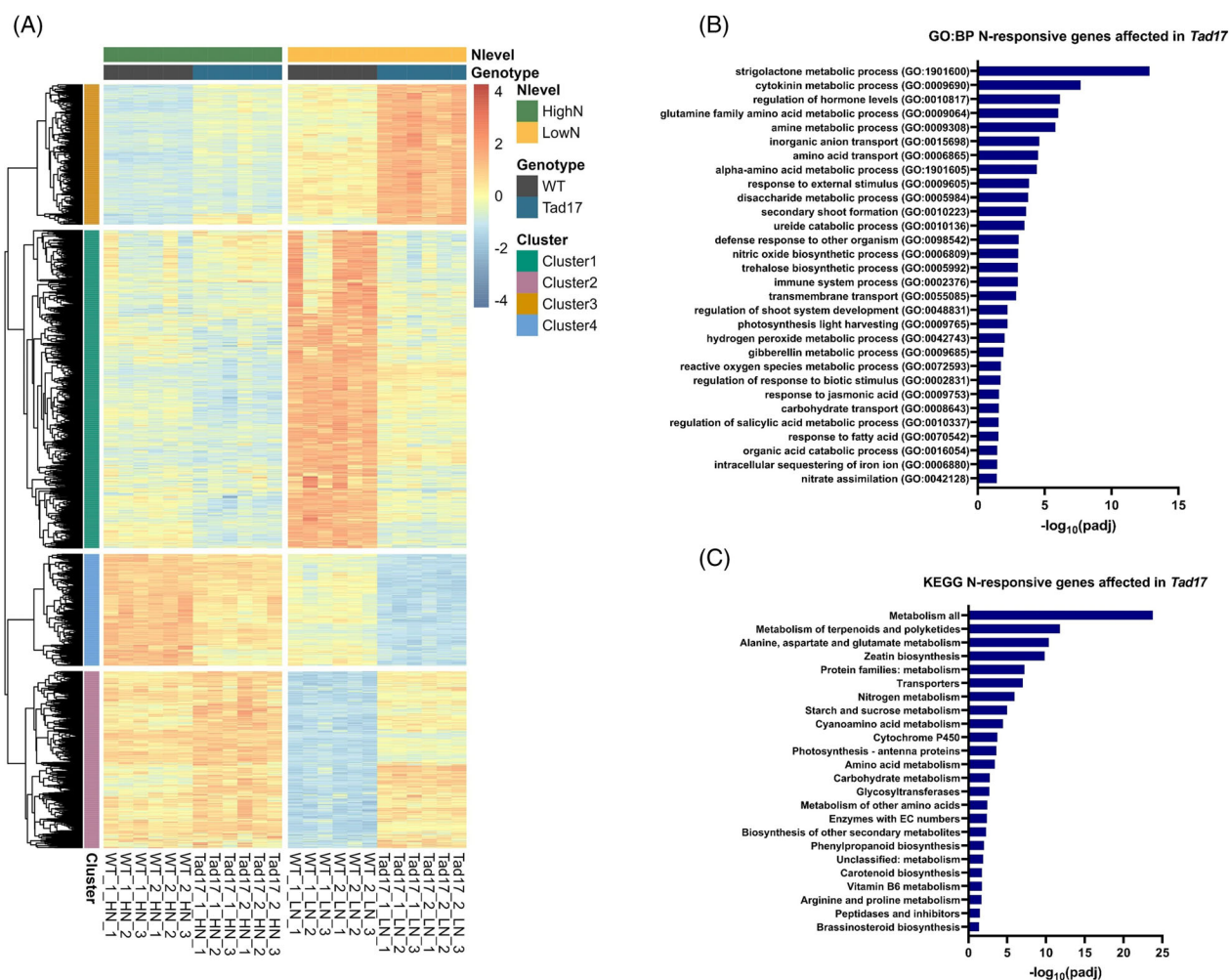
Figure 4. Altered transcriptional regulation of N-responsive genes in the basal nodes on *Tad17* in response to N limitation.
(A) Heatmap of N-responsive genes that were significantly differentially expressed in *Tad17* mutant under low N conditions compared with WT segregant. Each row corresponds to a different gene, while columns correspond to different samples grouped by treatment. Data are Z-scores of regularised log normalised counts (rlog) as generated by DESeq2. Warm colours correspond to higher transcript levels, while cold colours to lower levels. Row annotation corresponds to the four clusters identified based on the transcriptional response.
(B) Enriched GO: BP terms and (C) enriched KEGG terms among the differentially expressed N-responsive genes in the basal node of *Tad17* mutant under low N conditions.

overrepresented among genes in cluster 3 (Table S20). Amino acid breakdown is induced under N-limiting conditions, contributing to N recycling. *Tad17* mutants showed stronger expression of ureide catabolism, indicating that under N-limiting conditions, *Tad17* basal nodes were stronger N sinks compared with WT plants and showed higher levels of N recycling and reassimilation.

In addition, biological processes related to carbohydrate transport and metabolism were significantly affected by N limitation. Those changes may influence the sugar strength status of the tissue and thereby contribute to bud dormancy. GO terms such as 'disaccharide metabolic process' (GO:0005984) and 'carbohydrate transport' (GO:0008643), along with KEGG terms 'starch and sucrose

metabolism', were enriched among N-responsive genes found to be differentially expressed in *Tad17*. These findings suggest that *Tad17* showed imbalances in the regulation of carbon use and partitioning in response to nutritional signals.

**RNA-seq revealed changes in N-responsive TFs in *Tad17* basal nodes**

TFs are known to play an important role in regulating plant response to environmental stress by controlling the expression of many downstream genes. N limitation significantly affected the expression of 689 TFs in basal nodes. Most of the DE TFs, 478 (69%), were upregulated by N limitation, whereas 211 (31%) were found to be repressed by N

limitation. Further analysis revealed that 156 N-responsive TFs were found to be differentially expressed in *Tad17* compared with WT controls under low N, many of which showed a genotype-dependent response to N limitation (significant interaction between factors genotype and N level) (Table S22). Several studies have identified important TFs acting as master regulators controlling the expression of N-responsive genes (Gaudinier et al., 2018; Kiba et al., 2018; Ueda et al., 2020). Analysis of the expression of previously identified N master regulators showed that many of them were among the genes affected in *Tad17* under N-limiting conditions and showed a

genotype-dependent response to N limitation (Figure 5), implying an involvement of SLs in transcriptional regulatory networks in response to N limitation.

Tad17 mutants fail to downregulate CK synthesis and signalling under N limitation

Plant response to N limitation included significant changes in many genes involved in CK metabolism and signalling (Figure 6). Consistent with previous findings, the expression of CK biosynthetic genes was suppressed in the basal nodes of WT segregant plants in response to N limitation, while changes were also observed in genes involved in CK
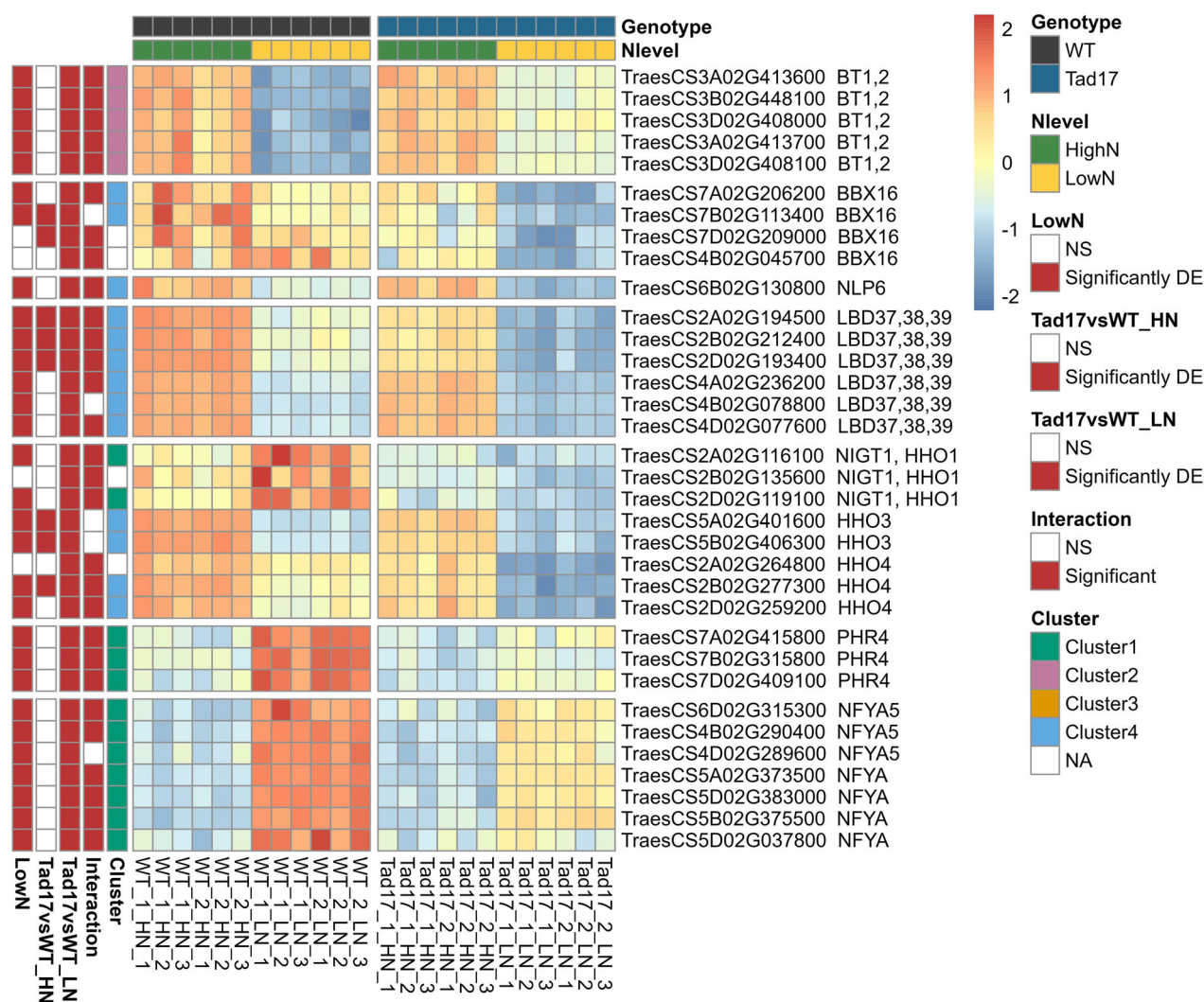
Figure 5. Transcriptional regulation of genes encoding transcription factors identified as master regulators of N response which were found to be differentially expressed in the basal node of *Tad17* mutant grown under low N conditions for 8 days.

Each row corresponds to a different gene, while columns correspond to different samples grouped by treatment. Data are Z-scores of regularised log normalised counts (rlog) as generated by DESeq2. Warm colours correspond to higher transcript levels, while cold colours to lower levels. Row names correspond to the gene ID and gene name of Arabidopsis orthologues. Row annotations indicate significant differential gene expression in N-limited nodes, in *Tad17* mutant under high N and in *Tad17* under low N conditions, significant interaction of genotype and N level, and cluster information based on the transcriptional response (from left to right).
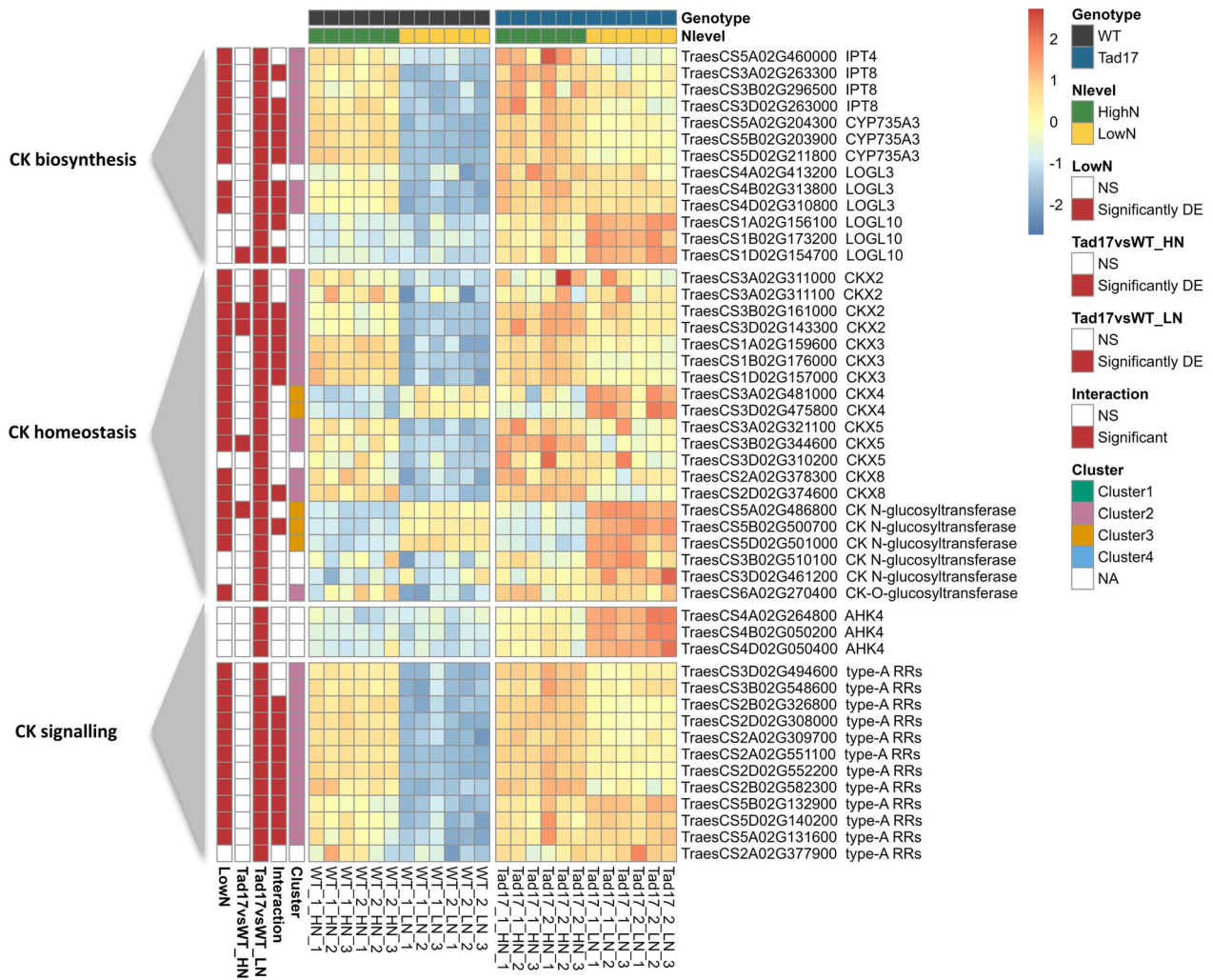
Figure 6. Transcriptional regulation of selected CK biosynthesis, homeostasis and signalling genes in the basal node of *Tad17* mutant and WT segregant grown under high N (10 mM) or low N (0.1 mM) conditions for 8 days.

Each row corresponds to a different gene, while columns correspond to different samples grouped by treatment. Data are *Z*-scores of regularised log normalised counts (rlog) as generated by DESeq2. Warm colours correspond to higher transcript levels, while cold colours to lower levels. Row names correspond to the gene ID and gene name. Row annotations indicate significant differential gene expression in N-limited nodes, in *Tad17* mutant under high N and in *Tad17* under low N conditions, significant interaction of genotype and N level and cluster information based on the transcriptional response (from left to right).

homeostasis and signalling. However, as shown in Figure 6, the transcript abundance of CK biosynthetic genes was significantly higher in nodes of *Tad17* compared with WT under N-limiting conditions, although not under N-abundant conditions. The differentially expressed biosynthetic genes included genes encoding ISOPENTENYL TRANSFERASE (IPT), CYP735A, and LONELY GUY (LOG) enzymes. IPTs catalyse the first step in CK biosynthesis, converting adenosine ribotides to isopentenyl adenosine ribotides (iPR), while CYP735A catalyses the formation of trans-Zeatin ribotide (tZR) from iPR, and LOG catalyses the conversion of both iP and tZ (the active CKs) from iPR and tZR (Kiba et al., 2023; Kurakawa et al., 2007; Takei, Ueda, et al., 2004; Takei, Yamaya, & Sakakibara,

2004). tZR is the main form of CK transported root-to-shoot, and is converted to active tZ at sites of perception to implement root-to-shoot signalling (Wheeldon & Bennett, 2021). Notably, the expression of CK biosynthesis genes was strongly repressed by N limitation in WT plants, but this repression was not observed in N-limited basal nodes of *Tad17*. Similarly, the expression of many CYTOKININ OXIDASE (CKX) encoding genes involved in CK degradation remained at high levels in *Tad17*, despite being strongly suppressed by N limitation in WT plants. The expression of genes encoding CK-glycosyltransferases involved in CK deactivation was also upregulated in *Tad17* compared with WT under N-limiting conditions. Additionally, although wheat homologues encoding HISTIDINE

KINASE4 (AHK4) CK receptor proteins were not among the N-responsive genes in WT, they were significantly upregulated induced in *Tad17* mutants under N-limiting conditions compared with WT, and upregulated in N-abundant conditions, although without significant differences. Finally, *A-TYPE RESPONSE REGULATOR* (RR) genes are CK-inducible genes and are used as molecular markers of CK signalling, while in Arabidopsis, it has been demonstrated that type-A RRs are required for branching control by CKs (Müller et al., 2015). Type-A RRs encoding genes were strongly downregulated under N-limiting conditions in WT due to lower levels of CKs, but were not downregulated in the *Tad17* mutant, indicating that CK signalling was not repressed in *Tad17* by N limitation. Therefore, SLs are required for the transcriptional regulation of CK metabolism and signalling in response to N limitation, as also suggested by the significant two-way interaction of factors genotype and N level for many of the above-mentioned genes (Figure 6).

Analysis of levels of different CK metabolites was conducted in the basal nodes to investigate the impact of N limitation and *Tad17* on CK levels (Figure 7; Table S23). Under high N conditions, no significant difference was observed in the concentrations of iP and iPR between the two genotypes. In response to N limitation, both iP and iPR concentrations exhibited a decrease in the WT. However, the *Tad17* mutant did not show a corresponding reduction in iP levels in response to N limitation. In fact, under N-limiting conditions, *Tad17* mutant plants exhibited a 1.7-fold higher iP concentration in the nodes compared with the WT. These observations suggest that SLs are required for N-mediated iP reduction, also supported by a significant two-way interaction ($F[1,10] = 6.59$, $P = 0.028$). However, this was not the case for iPR, as a similar reduction was observed in response to N limitation in both genotypes. In addition, this analysis revealed a pronounced reduction of both tZ and tZR in both genotypes in response to N limitation, consistent with the reduction of CK biosynthesis known to occur in low N conditions. Nevertheless, under both N regimes, *Tad17* mutants exhibited significantly higher accumulation of both tZ and tZR in the basal nodes compared with the respective control. Specifically, under high N supply, the tZR concentration was 1.4-fold higher ($t[5] = 3.02$, $P = 0.029$), and tZ was more than two-fold higher ($t[5] = 4.33$, $P < 0.01$) compared with the respective WT control. Similarly, under low N conditions, the tZR concentration was twofold higher in *Tad17* mutant nodes compared with the WT segregant ($t[6] = 10.9$, $P < 0.01$), while tZ was 1.8-fold higher ($t[6] = 3.83$, $P < 0.01$). The elevated accumulation of tZ and tZR in the basal nodes of the *Tad17* mutant may be associated with its increased tillering phenotype, as CKs are known to positively regulate tillering.
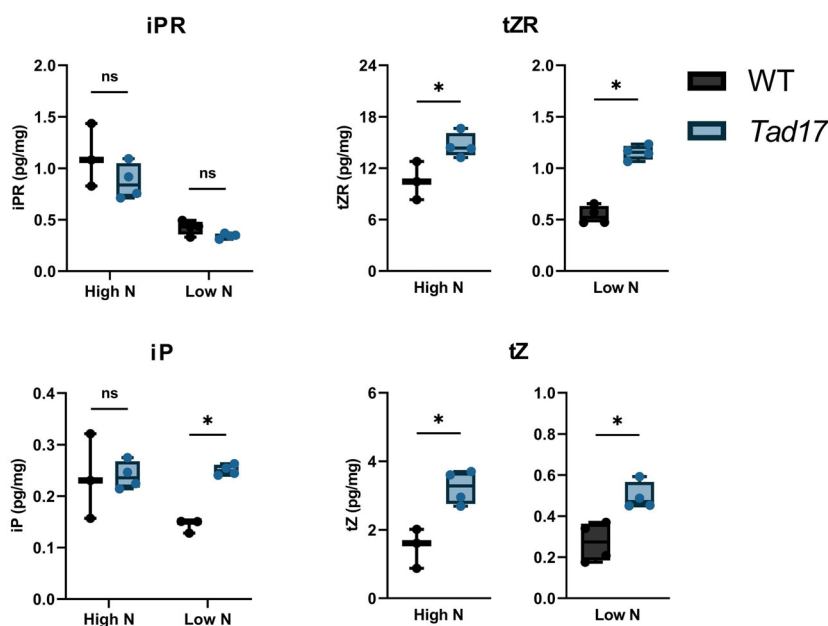
Figure 7. Concentration of CK metabolites in the basal node of *Tad17* mutant and WT segregant grown under high N (10 mᴍ) or low N (0.1 mᴍ) conditions for 8 days.
Values are means of four biological replicates, and error bars represent standard error. Statistical analysis was conducted with two-way ᴀɴᴏᴠᴀ (iPR, iP) or with independent samples *t*-test per N level (tZ and tZR). * and ns denote statistically significant differences and not significant differences between group means based on Tukey's HSD test (*P* = 0.05) or *t*-test (*P* < 0.05), respectively. iP, isopentenyl adenine; iPR, isopentenyl adenosine ribotide; tZ, trans-zeatin; tZR, trans-zeatin riboside.

DISCUSSION

Feedback regulation of SL synthesis and signalling

Although the role of SLs in tillering and other aspects of shoot growth regulation has been extensively studied in several species, the involvement of SLs in bread wheat growth has not been comprehensively demonstrated before. *Tad17* mutant lines showed a highly branched phenotype, suggesting that TaD17 and by extension, SLs are indeed involved in tillering regulation in wheat. *Tad17* mutants showed significant changes in SL biosynthetic gene expression, consistent with negative feedback regulation by SLs on their synthesis. In previous studies in Arabidopsis and rice, SL-deficient or SL-insensitive mutants have shown a strong upregulation of SL biosynthesis genes while the application of GR24, synthetic SL analogue, leads to downregulation of SL biosynthetic genes in SL-deficient mutant but not in SL signalling mutants (Arite et al., 2007; Mashiguchi et al., 2009; Umehara et al., 2008; Waters et al., 2012), implying that SL biosynthesis is controlled by the SL signalling pathway. Similar to the results presented in this work, strong upregulation of SL biosynthetic genes was seen in SL-deficient TaD27-RNAi wheat plants (Zhao et al., 2020). Intriguingly, we observed significant downregulation of *TaD53* homoeologues, which are the transcriptional repressors of the SL signalling pathway, in *Tad17* mutants. Similar results, showing positive feedback regulation of D53 by SLs, have previously been observed in rice (Song et al., 2017). These data suggest that under low SL conditions, plants sensitise themselves to SLs by reducing expression of the transcriptional repressors of SL signalling.

SLs coordinate shoot growth responses to N availability

Many studies have shown that SL induction is the main signal controlling shoot growth responses to soil P limitation, as SL-deficient and SL-insensitive mutants failed to control tillering in response to P supply (Kohlen et al., 2011; Umehara et al., 2010). However, the exact role of SLs in shoot growth regulation in response to N limitation has remained unclear, and in Arabidopsis, shoot growth responses to N are less dramatic than to P supply (De Jong et al., 2014; Kohlen et al., 2011) However, as shown in a previous study, wheat plants show higher sensitivity to N supply compared with P and SL synthesis is strongly induced by N limitation (Sigalas et al., 2023), and here, we observed that appropriate shoot growth responses to N limitation in wheat unambiguously require SL synthesis. Nevertheless, *Tad17* mutants responded to N limitation by changes in transcription and by reduced tiller numbers, and thus SLs are not the only signal contributing to tillering inhibition in response to N supply.

Given their systemic response to nutrient limitations, SLs are strong candidates for orchestrating transcriptional networks associated with nutrient limitations, driving important morphological and physiological adaptations to nutrient-deficient conditions. Interestingly, despite similar tillering phenotypes under both high and low N conditions, WT and *Tad17* exhibited more pronounced transcriptional differences under low N. This could be attributed to the role of SLs in coordinating plant responses to N limitation beyond tillering. This hypothesis is further supported by the observed transcriptional imbalance in *Tad17*, particularly in numerous N-responsive genes, including several master regulators of N response. The NIGT1/HHO family of GARP-G2-like TFs have a central role in N limitation response, while members of this family have also been found to control the balance between N and P metabolism (Kiba et al., 2018; Maeda et al., 2018; Ueda et al., 2020). In Arabidopsis BT1 and BT2 are known to suppress the expression of genes involved in N uptake and assimilation under N-sufficient conditions. (Araus et al., 2016), while several studies have also demonstrated that LBD37, LBD38, and LBD39 in Arabidopsis act as master regulators of the N response, maintaining the N deficiency response (Rubin et al., 2009). AtNF-YA5 also plays a pivotal role in regulating the transcriptional network in response to N availability signals in Arabidopsis (Gaudinier et al., 2018). In our study, genes encoding homoeologues of NIGT1, HHO3/4, BT1/2, LBD37/38/39, and NY-YA generally showed changes under N-limiting conditions that would be expected from previous studies, although the upregulation of NIGT1 in N-limited basal nodes of wheat was unexpected. Members of the NIGT1 subfamily are typically downregulated in Arabidopsis roots under N limitation, leading to the transcriptional activation of N starvation-responsive genes; the upregulation of NIGT1 in wheat might indicate a tissue-specific response to the N limitation in the basal nodes. Conversely, *Tad17* mutants revealed significant disruption to these transcriptional responses to N limitation, including a reduced downregulation BT1/2, over-downregulation of LBD37/38/39 and HHO3/4, a reduced upregulation of NIGT1 and NF-YAs (Figure 5). These results indicate a potential regulatory role of SLs in shaping plant responses to nutrient deficiencies. However, to fully elucidate the link between SLs and the observed changes in TF expression, further investigation is essential. Specifically, future research should aim to determine whether the alterations in TF expression are directly or indirectly influenced by SLs.

SLs and transcriptional responses in buds

Members of the *TB1* class of TCP TFs (BRC1 in Arabidopsis or FC1 in rice), have been shown to be involved in the regulation of shoot branching, and in several studies have been shown to be downstream target of the SL signalling pathway in eudicots (Aguilar-Martínez et al., 2007; Dun et al., 2012; Minakuchi et al., 2010). However, it has been

unclear whether the same connection between SLs and *TB1* exists in grasses. GR24 application does not affect the mRNA accumulation of *FC1*, while SL-deficient mutant did not show altered expression of *FC1* in rice (Arite et al., 2007; Minakuchi et al., 2010). Similarly, *TB1* expression in maize remained at high levels in highly branched SL-deficient plants (Guan et al., 2012). However, more recent studies showed that *FC1* expression was suppressed in SL-deficient and SL-insensitive rice mutants (Fang et al., 2020), and two recent studies showed that the application of GR24 induced the expression of *TB1/FC1* in rice tiller buds (Xu et al., 2015; Zha et al., 2022). Nevertheless, Zhao et al. (2020) reported that *TB1* expression was not affected in the D27-RNAi wheat mutants based on RNA-seq (Zhao et al., 2020). Our study further supports the argument that SLs do regulate *TB1* expression in grasses. Gene expression analysis in basal nodes by RT-qPCR showed that *TB1* levels were indeed suppressed in *Tad17*, and that the effect was more noticeable under N-limiting conditions. This observation is in favour of the model that SLs control tillering by affecting *TB1* expression.

Based on the transcriptional response to *TaTB1* in the *Tad17* mutant, a link between SLs and *TaTB1* in wheat is evident. However, this effect appears more pronounced under N-limiting conditions, raising questions about the underlying mechanism. Similarly, Bennett et al. (2016) suggested that TB1/BRC1 might not be required for bud dormancy per se but may be necessary for stabilising bud activity (Bennett et al., 2016); a concept that was subsequently supported by experimental evidence in Arabidopsis (Seale et al., 2017). Building upon this concept and the findings of our study, it is hypothesised that under conditions of adequate N supply, the regulatory role of TB1 in bud outgrowth may be diminished, with other signalling pathways such as auxin and sugar availability taking precedence in controlling bud outgrowth. Conversely, under N-limiting conditions, where resource availability is restricted, the regulation of tillering becomes crucial for plant survival and adaptation; therefore, SL-mediated regulation of *TB1* becomes more prominent.

SLs modulate CK homeostasis particularly in response to N signals

Collectively, our results demonstrate that SLs are not the only signal regulating shoot growth responses to soil N availability. Indeed, CKs are well-known signals of N availability that control tillering under N limitation (Sakakibara, 2021; Sakakibara et al., 2006). In our study, as expected, CK biosynthesis and CK levels showed a significant downregulation under N-limiting conditions (Figures 6 and 7). Since CKs act as positive regulators of tillering, the reduced accumulation of CKs, such as tZ and tZR, in the basal nodes contributes to tiller inhibition in wheat. Surprisingly, however, we observed that the response of

CK synthesis to N limitation strongly, although not completely, depended on intact SL synthesis. Thus, *Tad17* mutants did show a significant reduction in tZ and tZR levels in nodes in response to N limitation, which is likely to account for the residual reduction in tillering in *Tad17* under low N. CK biosynthesis and signalling are regulated by N availability through the NLP and NIGT1 TFs, as well as by glutamine-related signals connecting assimilated N with CK biosynthesis (Kamada-Nobusada et al., 2013; Maeda et al., 2018; Sakakibara, 2021). Thus, the altered expression of the N master regulatory pathways in the absence of SLs likely explains the failure to downregulate CK synthesis genes in *Tad17* mutants. Nevertheless, our results firmly place SLs upstream of CKs in the wheat response to N availability and show that SLs and CKs are not completely independent root-to-shoot signals for the regulation of shoot growth. A significant part of the negative effect of SLs on shoot branching in wheat under low N is thus likely mediated through the reduction in CK synthesis. Future analysis of SL and CK mutants would be valuable in fully elucidating the underlying mechanism and determining the contribution of different tiller inhibition mechanisms in response to N limitation.

In pea and Arabidopsis SL mutants showed no significant differences in CK levels in shoot tips (Foo et al., 2007), nor did *d10* rice mutants in shoot apices (Arite et al., 2007). However, more recent studies in rice have reported increased CK levels in tiller buds or plant bases of *d10* and *d53* mutants, consistent with the observation in *Tad17* basal nodes (Duan et al., 2019; Zhang et al., 2010). More specifically, *Tad17* showed elevated levels of tZ and tZR independently of plant N status, with these forms being the most abundant in wheat basal nodes. Consistent with our findings, a higher accumulation of tZ and tZR was also reported in shoot bases of rice *d53* mutants (Duan et al., 2019). Furthermore, a recent study demonstrated a reduction in CK levels in rice tiller buds upon application of GR24, a synthetic SL analogue (Zha et al., 2022), further supporting a suppressive effect of SLs on CK levels at shoot bases.

Despite the strong induction of CK biosynthesis genes, genes encoding CK catabolic and inactivation enzymes (such as CKX and CK glycosyltransferase) showed systematic induction in *Tad17* mutants under N-limiting conditions. The expression of CK catabolic enzymes is regulated by feedback mechanisms (Duan et al., 2019), suggesting that CK degradation might be strongly induced in *Tad17* mutants under low N conditions in response to elevated CK levels. The opposite might be true for CK biosynthesis genes, which are controlled by negative feedback regulation. We hypothesise that under high N conditions, the effect of SLs on CK biosynthetic genes is obscured by negative feedback regulation due to the high levels of CKs, whereas under low N conditions due to the overall reduction in CK levels, the feedback regulation is weaker, and the

effect of SLs becomes more apparent. This potential mechanism could explain the lack of a strong effect on CK biosynthetic genes in previous studies despite the increase in CK content. Additionally, a significant induction of CK signalling components was observed in *Tad17*. Therefore, it is likely that SLs also reduce sensitivity to CKs, which provides another mechanism for them to influence shoot branching. Consistent with this observation, Dun et al. (2012) reported that SL-deficient mutants are more sensitive to CKs than WT plants, and the application of GR24 reduces CK-induced growth in SL-deficient mutants but not in SL-insensitive mutants (Dun et al., 2012).

Consequently, we propose that SLs suppress CK levels by influencing CK biosynthesis and/or CK degradation, also play a role in sensitivity to CKs. However, other studies have demonstrated that CK levels also affect SL biosynthesis. SL biosynthetic genes are found to be suppressed after the application of CK in both root and basal nodes of rice plants (Xu et al., 2015). Moreover, CK application has been shown to reduce the levels of SLs in root exudates of sorghum, further supporting that CK has a negative effect on SL production (Yoneyama et al., 2020). Taken together, it is suggested that CK and SLs exhibit antagonistic actions in controlling plant architecture, while both are essential for plant adaptation to different N levels.

EXPERIMENTAL PROCEDURES

Tad17 triple knock-out mutant generation

For the generation of *Tad17* triple knock-out mutant, mutant lines with nonsense mutation in *TaD17-2A* (TraesCS2A02G414600), *TaD17-2B* (TraesCS2B02G433800) and *TaD17-2D* (TraesCS2D02G411900) were selected from hexaploid wheat, *T. aestivum* cv Cadenza, TILLING population (Krasileva et al., 2017) (Table S1). Line Cad1738 carries a mutation at nucleotide 539 in *Tad17-2A* transcript leading to a truncated protein of 455 amino acids. Cad1271 carries a G to A substitution at nucleotide 1275 of *TaD17-2B* leading to a premature coding at position 425. Finally, Cad0880 shows a deletion of 132 amino acids from the C-terminus of *TaD17-2D*. Truncated proteins are lacking important amino acid residues for the functionality of CCD7/D17 suggesting non-functional enzymes (Harrison & Bugg, 2014; Messing et al., 2010) (Figure S1). For the generation of triple knock-out mutant plants, a crossing scheme was followed to stack the nonsense mutant alleles. One round of backcrossing to non-mutagenized cv. Cadenza was conducted to reduce the background mutation load. The crossing scheme followed is summarised in Figure S2. *Tad17* triple homozygous plants (aabbdd) and wild-type (WT, AABBDD) sibling lines were obtained and used for further experimentation.

Genotyping

TILLING mutant lines were genotyped by either sequencing the flanking region of the mutation site or by using Kompetitive allele-specific PCR assays (KASP). Genomic DNA was extracted from wheat seedling leaf samples. The extraction method involved lyophilization in a Modulyo freeze dryer (Edwards, West Sussex, UK), grinding with 3 mm stainless steel beads using the Geno/Grinder 2010 (SPEX SamplePrep, Metuchen, NJ, USA), followed

by incubation in extraction buffer (100 mM TrisBase, 1 M KCL, and 10 mM EDTA, pH 9.5) at 65°C for 1 h. Cell debris was removed by adding 330 μl of potassium acetate (5 M), mixing, and centrifugation. The supernatant was transferred to a fresh microcentrifuge tube and DNA was precipitated with 550 μl isopropanol. Pelleted DNA was washed with 75% (v/v) EtOH and resuspended in 200 μl of TE buffer (10 mM Tris–HCl pH 7.5, 0.1 mM EDTA). For high-throughput extraction, a modified protocol using 96-deep well plates (Thermo Scientific, Waltham, MA, USA) was used by adjusting volumes and incubation times accordingly.

For genotyping by sequencing homoeologue-specific primers were designed to amplify the region that contains the mutation site (Table S2). PCR was performed with a Touchgene Gradient PCR machine (Techne, Staffordshire, UK), using Q5 high-fidelity DNA polymerase (New England BioLabs, Ipswich, MA, USA) following the manufacturer's protocol. After the amplification of the targeted region, PCR products were purified with the Wizard SV Gel and PCR Clean-Up System (Promega, Madison, WI, USA), following the manufacturer's protocol. The PCR products were sequenced using the TubeSeq service (Eurofins Genomics, Luxemburg, Luxemburg).

KASP genotyping was utilised for high-throughput genotyping. SNP-specific KASP primers were manually designed, with the SNP at the 3′ end of the primer. FAM and VIC probe sequence to the 5′ end of the WT- and mutant-allele-specific KASP primer, respectively (Table S3). KASP assays were performed in an ABI-7500 real-time PCR system (Applied Biosystems, Waltham, MA, USA) using a PACE Low-ROX mix (3CR Bioscience, Harlow, UK). Each reaction was prepared by pipetting 2 μl of extracted DNA (around 50 ng μl^{-1}) in a white 96-well qPCR Plate (4titude, Surrey, UK) and then by adding 0.14 μl of KASP primer mix (12 μM KASP primer 1, 12 μM KASP primer 2, 30 μM KASP primer 3), 2.86 μl H$_2$O and 5 μl PACE Row-ROX mix prepared as a master mix. The plate was sealed with an adhesive qPCR seal (4titude, Surrey, UK), and after a short shaking and short centrifugation, the plate cycled in the AB-7500. The PCR cycling parameters used were 15 min at 94°C, 10 cycles at 94°C for 20 sec and 68°C (−0.6°C per cycle) for 60 sec, followed by 32–40 cycles at 94°C for 20 sec and 62°C for 60 sec. Finally, the plate reading was performed at 30°C for 60 sec. The data were analysed with the allelic discrimination function for genotyping as implemented in the software ABI 7500 v2.0.6 (Applied Biosystems, Waltham, MA, USA).

Hydroponic culture of wheat

Plants were cultured in a custom hydroponic system in a controlled environment chamber. Seeds were surface sterilised with 1:40 bleach solution: dH$_2$O (v/v) for 15 min, followed by five washes with sterilised dH$_2$O. Seeds were soaked in sterilised dH$_2$O overnight at 4°C in the dark. Subsequently, seeds were placed in black boxes with wet filter paper to germinate (Day 0). Individual plants were grown held by foam buds on top of 1 L black pots containing the nutrient solution. The nutrient solution was aerated throughout the experiment by an aeration pump tubing system. The growing conditions were 20/10°C day and night temperature, respectively, and 14 h day length. Lighting was provided by fluorescent bulbs at an intensity of 550 μmol m^{-2} sec^{-1}. The humidity was 65% during the day and 75% during the night. Seedlings were transferred to the hydroponic culture system 4 days after sowing (DAS). All genotypes were supplied with half-strength nutrient solution for the initial 3 days (until 7 DAS) and then supplied with full-strength nutrient solution. The composition of the basic nutrient solution, modified Letcombe (Drew & Saker, 1984), was 1.5 mM Ca(NO$_3$)$_2$, 5 mM KNO$_3$, 2 mM NaNO$_3$, 1.5 mM MgSO$_4$, 1 mM

phosphate buffer solution (KH_2PO_4, pH 6.0), 50 μM FeNaEDTA, 0.5 μM $CuCl_2$, 20 μM H_3BO_3, 3.6 μM $MnCl_2$, 0.1 μM Na_2MoO_4 and 0.77 μM $ZnCl_2$. In addition, 2.35 mM MES monohydrate was added as a buffer and the pH was adjusted to 5.8 with KOH. The nutrient solution was renewed every 3–4 days. For Low N treatment, plants were supplied with 0.1 mM of N in the form of KNO_3. For ionic balance in the low N nutrient solution, $Ca(NO_3)_2$ was replaced by $CaCl_2$, KNO_3 by KCl_2, and $NaNO_3$ by NaCl.

Experimental design

Tad17 triple homozygous knock-out mutant (aabbdd) and wild-type (AABBDD) sibling lines (also referred to as WT segregant) were grown hydroponically. Plants from two BC_1F_3 populations for each genotype, from two self-pollinated *Tad17* mutants and two WT segregant lines, were grown with three replicates per treatment (Figure S3). In other words, six biological replicates per genotype were included consisting of three biological replicates per line within the same genotype. Analysis of two segregating lines per genotype was selected as an approach to rule out any effects caused by unlinked mutations (Uauy et al., 2017).

An incomplete Trojan square design was used for this experiment. All genotypes (WT, *Tad17*) received full-strength nutrient solution until 10 DAS. At 10 DAS, half of the plants per line were supplied with Low N nutrient solution (0.1 mM N), while the rest of the plants continued receiving High N nutrient solution (10 mM N). Sampling took place at 18 DAS, 8 days after the introduction of the plants to N limitation. Each biological replicate consisted of tissue material from three plants pooled together to ensure enough material for downstream analysis. Another sampling was conducted at 22 DAS for plant biomass measurements. For the latter, a single plant was harvested per biological replicate.

Plant phenotypic measurements

The number of outgrown tillers per plant was recorded at different time points, depending on the experimental design. Only tillers that had emerged from the leaf sheath were recorded. For the determination of root and shoot biomass, whole root and shoot samples were freeze-dried in Modulyo freeze dryer (Edwards, West Sussex, UK) for at least 2 days, and then the dry weight of each tissue was recorded.

The chlorophyll content of leaves was measured using the SPAD-502 chlorophyll meter (Konica Minolta, Tokyo, Japan). Measurements were taken from three distinct positions along the length of the leaf under examination. The average value derived from these readings was then recorded as the representative proxy for the chlorophyll content of each leaf.

Tissue harvesting/sampling

In the context of this study, the 'basal node' was characterised as the proximal 0.5 cm segment of the main shoot base, which includes the shoot apical meristem, any dormant lateral buds present, and the leaf meristems. Sample preparation involved the removal of the entire root system from the shoot and any primary tillers that had outgrown and emerged from the leaf sheath. Subsequently, the basal 0.5 cm of the main shoot was dissected, immediately frozen in liquid nitrogen, and stored at −80°C before further processing.

RNA extraction

Tissue samples were ground to a fine powder in liquid nitrogen. Basal node samples were hand-ground with pre-cooled mortar and pestle. Total RNA was extracted from 100 mg of basal node tissue by using the RNeasy Plant Mini Kit (Qiagen, Hilden, Germany) following the manufacturer's instructions. Elution of the column was performed with 50 μl RNase-free H_2O. DNase treatment, phenol/chloroform/isoamyl-alcohol purification steps, and RNA precipitation were conducted as described by Sigalas et al. (2023).

The concentration of the extracted RNA was determined by the Qubit Broad Range assay (Invitrogen, Waltham, MA, USA), while A280/A260 measured using the Nanodrop 2000 spectrophotometer (Thermo Scientific, Waltham, MA, USA) was used as a quality check of the extracted RNA. The quality of the extracted RNA was also evaluated by running 500 ng of RNA in 1% agarose TAE-gel.

High-throughput RNA-sequencing

A total of 2–3 μg of RNA samples were submitted for next-generation sequencing. Prior to the library preparation, RNA integrity was assessed with the RNA kit on Aligent 5300 Fragment Analyser. Quality control, poly-A selection for rRNA removal, library preparation, multiplexing and sequencing were performed by Genewiz UK (Takeley, UK) according to their standard workflow. Briefly, RNA library preparation was prepared using the NEBNext Ultra II Library Prep Kit for Illumina, following the manufacturer's protocol. First, oligo-dt beads were used for mRNA enrichment, and the mRNAs were fragmented for 15 min at 94°C. First and second-strand cDNA were subsequently synthesised. Indexed adapters were ligated to cDNA fragments after adenylation of the 3′ end of the cDNA fragments. Limited cycle PCR was used for library amplification. Sequencing libraries were validated using the NGS Kit on the Agilent 5300 Fragment Analyser and quantified by using a Qubit 4.0 Fluorometer or equivalent. The sequencing libraries were multiplexed and loaded on the flow cell. Next-generation sequencing was performed in Illumina Novaseq 6000 with 2 × 150 bp pair-end configuration v1.5. Image analysis and base calling were conducted by the NovaSeq Control Software v1.7 on the NovaSeq instrument. Raw paired-end data were delivered in fastq format after de-multiplexing and standard adapter trimming by the sequencing contractor. One mismatch was allowed for index sequence identification.

RNA-sequencing data analysis workflow

All the tools used for the RNA-seq data analysis were executed in the Rothamsted Research Galaxy platform (https://galaxy.rothamsted.ac.uk/) unless stated otherwise. *FastQC v0.11.7* tool was used to assess the quality of the raw data (http://www.bioinformatics.babraham.ac.uk/projects/fastqc/). Low-quality reads and adapter sequences were removed using *Cutadapt v3.7* (Martin, 2011). Subsequently, trimmed reads were mapped to *T. aestivum* reference genome IWGSC RefSeq v1.0 using the tool *HISAT2 v2.2.1* (Kim et al., 2015). The *featureCounts* tool was used for assigning mapped reads to exons and counting the number of mapped reads per annotated gene using RefSeq Annotation v1.1 (Liao et al., 2014). RefSeq1.1 contains in total 107 891 high-confidence (HC) genes and 161 537 low-confidence (LC) genes. HC genes correspond to HC protein-coding loci with a predicted function, whereas LC genes correspond to partially supported gene models, gene fragments, and gene orphans. Evidence for transcription has been found for 85% (94 114) of the HC genes, whereas LC showed much lower evidence of transcription of just 49% (Appels et al., 2018). *DESeq2* package was used to perform the differential gene expression analysis (alpha = 0.01) by fitting the appropriate model based on each experimental design (Love et al., 2014). A prefiltering of low-count genes was performed

before performing differential gene expression analysis. Only genes that had at least three samples with more than five reads were included in the analysis. Significantly DEG were retrieved by applying post hoc filtering of *P*-value adjusted for multiple comparisons (*P*adj) <0.01 and |log$_2$fold change (FC)| >0.58 (|FC| > 1.5). The package *DEGreport v1.38.5* and its function degPatterns were used to cluster genes based on their expression patterns across treatment combinations (Lorena Pantano, 2023). In addition to the above workflow, raw reads were also pseudo-aligned to IWGSC RefSeq v1.0 annotation v1.1 using Kallisto v0.46.0.4 (Bray et al., 2016). The package *tximport v1.24.0* was used to create gene-level abundance from the transcript abundances (Soneson et al., 2015). The *DESeq2*, *DEGreport*, and *tximport* packages were run in R Statistical Software v4.1.1 on a local Windows machine.

For the biological interpretation of the data, GO enrichment analysis was performed in *g: Profiler* using the *g: GOst* tool and default parameters (statistical domain scope: only annotated genes, multiple testing correction: g: SCS algorithm, *P*adj <0.05) (Raudvere et al., 2019). REVIGO web server was used to summarise the enrichment analysis results by removing redundant terms (Supek et al., 2011). Oligopeptide sequences of the DEGs were retrieved from BioMart in FASTA format. KEGG Orthology (KO) annotations for the DEGs were retrieved using the BlastKoala tool (https://www.kegg.jp/blastkoala/). In addition, pathway enrichment analysis was conducted in g: GOst tool against a custom *T. aestivum* KEGG reference containing more than 46 000 wheat genes covering both KEGG pathways and BRITE hierarchies. Finally, *g: Orth* tool in *g: Profiler* was used for retrieving orthologue genes of the DEGs in rice and Arabidopsis.

RT-qPCR and RNA-seq validation

First-strand cDNA was synthesised from 2 μg of total RNA using SuperScript III Reverse Transcriptase (Invitrogen, Waltham, MA, USA) and oligo(dT) primers following the manufacturer's instructions.

TaTB1 expression analysis was performed by RT-qPCR. The real-time qPCRs were performed in an ABI-7500 real-time PCR system (Applied Biosystems, Waltham, MA, USA) using SYBR® Green JumpStart™ Taq ReadyMix™ (Sigma-Aldrich, Dorset, UK) with two technical replications. The gene expression levels were calculated as normalised relative quantity (NRQ) as described by Sigalas et al. (2023). Wheat actin3 (*TaACT3*) and succinate dehydrogenase (*TaSDH*) genes were used as reference genes. Primer sequences can be found in Table S4.

Additionally, *TaCKX3*, *TaD10*, *TaD14*, *TaGS1*, *TaNR1*, and *TaSUS2* were used for RNA-seq validation, by comparing the gene transcript abundance (TPM) with the NRQ value obtained from RT-qPCR (Table S4). Pearson correlation between transcript abundance values of selected genes obtained from the RNA-seq and RT-qPCR was performed using package ggpubr v0.4.0 in R Statistical Software v4.1.1 on a local Windows machine. For all six genes, there was a good correlation (*R* > 0.9) between the expression values obtained from the RNA-seq and the RT-qPCR, suggesting that the RNA-seq data were reliable (Figure S4).

Cytokinin extraction and quantification

Cytokinins were extracted from 20 mg of ground plant tissue using a 70:29:10 (v/v/v) methanol:water:formic acid solution containing 0.2 ng ml^{-1} each of D-iP, D-iPR, D-tZ, D-DHZ, and D-DHZR as internal standards. Samples were homogenised in a mixer mill MM400 for 1 min at 30 Hz with two metal beads, followed by 30 min incubation at 4°C on a vortex. After centrifugation, supernatants were collected and evaporated under N$_2$ on SPE Dry 96

(Biotage, Uppsala, Sweden). The pellet was resuspended in 800 μl of 2% formic acid in ddH$_2$O and subjected to filtration and solid-phase extraction using an Extrahera system (Biotage, Uppsala, Sweden) using Isolute Filter Plates 25 μm/0.2 μm (Biotage) and Evolute CX express 30 mg/1 ml columns (Biotage, Uppsala, Sweden). The eluate was evaporated, and the pellet was resuspended in 100 μl of 0.1% formic acid.

Analysis of CK metabolites (isopentenyl adenine [iP]; isopentenyl adenosine [iPR]; trans-zeatin [tZ]; tZ-riboside [tZR]; cis-zeatin [cZ]; cZ-riboside [cZR]) was conducted by UHPLC–MS/MS using a Nexera X2 UHPLC system coupled to a QTRAP 6500+ mass spectrometer (Sciex, Concord, Canada). Separation was achieved with a Kinetex Evo C18 column at a flow rate of 0.7 ml min^{-1}. The mobile phase consisted of solvent A (H$_2$O: 0.1% formic acid) and solvent B (ACN: 0.1% formic acid) and a 0.7 ml min^{-1} flow rate. The optimised linear gradient system was: 0–3 min, 20% B; 3–4 min, 25% B; 4–4.5 min, 100% B; 4.5–6 min, 100% B; 6–6.5 min, 2% B and 6.5–8.6 min, 2% B. The concentration of CK metabolites was calculated based on peak area ratios relative to internal standards using standard curves constructed from dilution series of each of the examined CKs.

Visualisation

Figures and graphs were created in GraphPad Prism v9.3.1 for Windows (San Diego, CA, USA). Package *pheatmap v1.0.12* and *ggplot2 v3.3.6* were also used in R Statistical Software v4.1.1 on a local Windows machine for the generation of heatmaps and some graphs.

Statistical analysis

Mean values and standard errors were calculated from at least four biological replicates, depending on the experimental design. The exact number of biological replicates is mentioned in each figure legend. The statistically significant effects of the treatments/factors were assessed with either ANOVA or *t*-test where applicable. Statistical analyses were conducted using the GenStat statistical software package (21st edition) or the package *rstatix v0.7.0* R Statistical Software v4.1.1 on a local Windows machine. Repeated measures ANOVA was conducted for SPAD dynamic data. Prior to ANOVA, assumptions for normality and homogeneity of variances were assessed using Shapiro–Wilk's normality test and Levene's test, respectively. If the data did not meet the normality assumption, appropriate transformations were applied. In cases where the assumption of homogeneity of variances was violated (Levene's test *P* < 0.05, such as with tZ and tZR), group mean comparisons were conducted using *t*-tests. Following ANOVA, Tukey's Honest Significant Difference test at a significance level of 5% (*P* = 0.05) was performed to conduct pairwise comparisons and identify significant differences between group means.

AUTHOR CONTRIBUTIONS

PPS and MJH: conceptualization; PPS: formal analysis; PPS: investigation; PPS: data curation; PPS and TB: writing – original draft; PB, SGT, FJ, MA, J-CY, MJB, and MJH: writing – review; PPS: revision, PPS: visualisation; FJ, MJB, and MJH: supervision.

ACKNOWLEDGEMENTS

CONFLICT OF INTEREST

No conflict of interest was declared.

DATA AVAILABILITY STATEMENT

All data supporting the findings of this study are available within the paper and within its supporting materials published online. The raw data from RNA-seq are available at the ArrayExpress (E-MTAB-14014).

SUPPORTING INFORMATION

Additional Supporting Information may be found in the online version of this article.

Data S1. Gene transcript abundance (expressed as TPM) in the basal node of *Tad17* and WT segregant grown hydroponically under high or low N conditions.

Figure S1. Protein alignment of members of the CCD/CCO family from diverse plant species, including WT and truncated TaD17-2A, -2B and -2D.

Figure S2. Crossing scheme used to stack the selected mutant alleles of all the *TaD17* homoeologues.

Figure S3. Schematic representation of WT and *Tad17* mutant lines used in the hydroponic experiment.

Figure S4. RNA-seq validation test results.

Figure S5. (a) Number of shoots at ear emergence and (b) number of ears at final harvest per plant in triple *Tad17* mutants and WT segregant lines.

Figure S6. (a) Principal component analysis based on the RNA-seq data analysis results of genotype (*Tad17*, WT) and N treatment (High N, Low N) effects. PCA was based on the 1000 most variable genes. (b) Sample distance matrix based on the RNA-seq. (c) Volcano plot of the differential gene expression analysis of N limitation effect in WT and (d) *Tad17* mutant.

Figure S7. Sub-clustering of N-responsive genes that were significantly differentially expressed in *Tad17* mutant under low N conditions compared with WT segregant using the DEGpattern function of DEGreport package.

Table S1. TILLING mutant line IDs with a stop-gained mutation in the protein-coding region of *TaD17* homoeologues.

Table S2. Homoeologue-specific primers used for the genotyping of the mutant lines by sequencing.

Table S3. Primer sequences designed and used for KASP genotyping of the mutant alleles.

Table S4. Forward and reverse primer sequences used in the RT-qPCR.

Table S5. Phenotypic data of *Tad17* and WT plants grown hydroponically under high or low N conditions.

Table S6. RNA-sequencing raw data analysis statistics.

Table S7. Significantly differentially expressed genes (*P*adj < 0.01 and |FC| > 1.5) in response to N limitation in WT segregant plants.

Table S8. Significantly differentially expressed genes (*P*adj < 0.01 and |FC| > 1.5) in response to N limitation in *Tad17* mutant.

Table S9. Significantly differentially expressed genes (*P*adj < 0.01 and |FC| > 1.5) in *Tad17* mutant compared with WT under high N.

Table S10. Significantly differentially expressed genes (*P*adj < 0.01 and |FC| > 1.5) in *Tad17* mutant compared with WT under low N.

Table S11. List of genes showing significant 2-way interaction between factors genotype and N level based on DESeq2 (*P*adj < 0.01).

Table S12. GO-enriched terms in the DE genes in the basal node of *Tad17* mutant compared with WT under high N conditions.

Table S13. GO-enriched terms in the DE genes in the basal node of *Tad17* mutant compared with WT under low N conditions.

Table S14. KEGG-enriched terms in the DE genes in the basal node of *Tad17* mutant compared with WT under high N conditions.

Table S15. KEGG-enriched terms in the DE genes in the basal node of *Tad17* mutant compared with WT under low N conditions.

Table S16. *TaTB1* normalised relative quantity (NRQ) data based on the RT-qPCR expression analysis.

Table S17. List of N-responsive genes that were significantly differentially expressed in *Tad17* mutant compared with WT segregant under low N conditions.

Table S18. GO-enriched terms in the N-responsive genes affected in *Tad17* mutant compared with WT under low N conditions.

Table S19. KEGG-enriched terms in the N-responsive genes affected in *Tad17* mutant compared with WT under low N conditions.

Table S20. GO-enriched terms in each cluster of N-responsive genes affected in *Tad17* mutant compared with WT under low N conditions.

Table S21. KEGG-enriched terms in each cluster of N-responsive genes affected in *Tad17* mutant compared with WT under low N conditions.

Table S22. Differential gene expression analysis results of N-responsive TF that were found to be differentially expressed in N-limited *Tad17* basal nodes compared with WT control.

Table S23. Concentration of CK metabolites (pg/mg) in the basal node of *Tad17* mutant and WT segregant grown under high N or low N conditions for 8 days.

REFERENCES

Abe, S., Sado, A., Tanaka, K., Kisugi, T., Asami, K., Ota, S. *et al.* (2014) Carlactone is converted to carlactonoic acid by MAX1 in Arabidopsis and its methyl ester can directly interact with AtD14 in vitro. *Proceedings of the National Academy of Sciences of the United States of America*, **111**, 18084–18089.

Aguilar-Martínez, J.A., Poza-Carrión, C. & Cubas, P. (2007) Arabidopsis BRANCHED1 acts as an integrator of branching signals within axillary buds. *Plant Cell*, **19**, 458–472.

Araus, V., Vidal, E.A., Puelma, T., Alamos, S., Mieulet, D., Guiderdoni, E. *et al.* (2016) Members of BTB gene family of scaffold proteins suppress nitrate uptake and nitrogen use efficiency. *Plant Physiology*, **171**, 1523–1532.

Arite, T., Iwata, H., Ohshima, K., Maekawa, M., Nakajima, M., Kojima, M. *et al.* (2007) DWARF10, an RMS1/MAX4/DAD1 ortholog, controls lateral bud outgrowth in rice. *Plant Journal*, **51**, 1019–1029.

Barbier, F.F., Dun, E.A., Kerr, S.C., Chabikwa, T.G. & Beveridge, C.A. (2019) An update on the signals controlling shoot branching. *Trends in Plant Science*, **24**, 220–236.

Bennett, T. & **Leyser, O.** (2014) Strigolactone signalling: standing on the shoulders of DWARFs. *Current Opinion in Plant Biology*, **22**, 7–13.

Bennett, T., **Liang, Y.**, **Seale, M.**, **Ward, S.**, **Müller, D.** & **Leyser, O.** (2016) Strigolactone regulates shoot development through a core signalling pathway. *Biology Open*, **5**, 1806–1820.

Bray, N.L., **Pimentel, H.**, **Melsted, P.** & **Pachter, L.** (2016) Near-optimal probabilistic RNA-seq quantification. *Nature Biotechnology*, **34**, 525–527.

Brewer, P.B., **Yoneyama, K.**, **Filardo, F.**, **Meyers, E.**, **Scaffidi, A.**, **Frickey, T.** *et al.* (2016) Lateral branching oxidoreductase acts in the final stages of strigolactone biosynthesis in Arabidopsis. *Proceedings of the National Academy of Sciences of the United States of America*, **113**, 6301–6306.

Chesterfield, R.J., **Vickers, C.E.** & **Beveridge, C.A.** (2020) Translation of strigolactones from plant hormone to agriculture: achievements, future perspectives, and challenges. *Trends in Plant Science*, **25**, 1087–1106.

Clark, J. & **Bennett, T.** (2024) Cracking the enigma: understanding strigolactone signalling in the rhizosphere. *Journal of Experimental Botany*, **75**, 1159–1173.

De Jong, M., **Ongaro, V.** & **Ljung, K.** (2014) Auxin and strigolactone signalling are required for modulation of Arabidopsis shoot branching by nitrogen supply. *Plant Physiology*, **166**, 384–395.

Drew, M.C. & **Saker, L.R.** (1984) Uptake and long-distance transport of phosphate, potassium and chloride in relation to internal ion concentrations in barley: evidence of non-allosteric regulation. *Planta*, **160**, 500–507. Available from: https://doi.org/10.1007/BF00411137

Duan, J., **Yu, H.**, **Yuan, K.**, **Liao, Z.**, **Meng, X.**, **Jing, Y.** *et al.* (2019) Strigolactone promotes cytokinin degradation through transcriptional activation of CYTOKININ OXIDASE/ DEHYDROGENASE 9 in rice. *Proceedings of the National Academy of Sciences of the United States of America*, **116**, 14319–14324.

Dun, E.A., **Germain, A.d.S.**, **Rameau, C.** & **Beveridge, C.A.** (2012) Antagonistic action of strigolactone and cytokinin in bud outgrowth control. *Plant Physiology*, **158**, 487–498.

Fang, Z., **Ji, Y.**, **Hu, J.**, **Guo, R.**, **Sun, S.** & **Wang, X.** (2020) Strigolactones and brassinosteroids antagonistically regulate the stability of the D53–OsBZR1 complex to determine FC1 expression in rice tillering. *Molecular Plant*, **13**, 586–597.

Fichtner, F., **Barbier, F.F.**, **Annunziata, M.G.**, **Feil, R.**, **Olas, J.J.**, **Mueller-Roeber, B.** *et al.* (2021) Regulation of shoot branching in Arabidopsis by trehalose 6-phosphate. *New Phytologist*, **229**, 2135–2151.

Fichtner, F., **Barbier, F.F.**, **Feil, R.**, **Watanabe, M.**, **Annunziata, M.G.**, **Chabikwa, T.G.** *et al.* (2017) Trehalose 6-phosphate is involved in triggering axillary bud outgrowth in garden pea (*Pisum sativum* L.). *Plant Journal*, **92**, 611–623.

Figueroa, C.M., **Feil, R.**, **Ishihara, H.**, **Watanabe, M.**, **Kölling, K.**, **Krause, U.** *et al.* (2016) Trehalose 6-phosphate coordinates organic and amino acid metabolism with carbon availability. *Plant Journal*, **85**, 410–423.

Foo, E., **Morris, S.E.**, **Parmenter, K.**, **Young, N.**, **Wang, H.**, **Jones, A.** *et al.* (2007) Feedback regulation of xylem cytokinin content is conserved in pea and Arabidopsis. *Plant Physiology*, **143**, 1418–1428.

Gaudinier, A., **Rodriguez-Medina, J.**, **Zhang, L.**, **Olson, A.**, **Liseron-Monfils, C.**, **Bågman, A.M.** *et al.* (2018) Transcriptional regulation of nitrogen-associated metabolism and growth. *Nature*, **563**, 259–264.

Guan, J.C., **Koch, K.E.**, **Suzuki, M.**, **Wu, S.**, **Latshaw, S.**, **Petruff, T.** *et al.* (2012) Diverse roles of strigolactone signaling in maize architecture and the uncoupling of a branching-specific subnetwork. *Plant Physiology*, **160**, 1303–1317.

Harrison, P.J. & **Bugg, T.D.H.** (2014) Enzymology of the carotenoid cleavage dioxygenases: reaction mechanisms, inhibition and biochemical roles. *Archives of Biochemistry and Biophysics*, **544**, 105–111.

Jiang, L., **Liu, X.**, **Xiong, G.**, **Liu, H.**, **Chen, F.**, **Wang, L.** *et al.* (2013) DWARF 53 acts as a repressor of strigolactone signalling in rice. *Nature*, **504**, 401–405.

Kamada-Nobusada, T., **Makita, N.**, **Kojima, M.** & **Sakakibara, H.** (2013) Nitrogen-dependent regulation of de novo cytokinin biosynthesis in rice: the role of glutamine metabolism as an additional signal. *Plant & Cell Physiology*, **54**, 1881–1893.

Kebrom, T.H., **Spielmeyer, W.** & **Finnegan, E.J.** (2013) Grasses provide new insights into regulation of shoot branching. *Trends in Plant Science*, **18**, 41–48.

Kiba, T., **Inaba, J.**, **Kudo, T.**, **Ueda, N.**, **Konishi, M.**, **Mitsuda, N.** *et al.* (2018) Repression of nitrogen starvation responses by members of the Arabidopsis GARP-type transcription factor NIGT1/HRS1 subfamily. *Plant Cell*, **30**, 925–945.

Kiba, T., **Mizutani, K.**, **Nakahara, A.**, **Takebayashi, Y.**, **Kojima, M.**, **Hobo, T.** *et al.* (2023) The trans-zeatin-type side-chain modification of cytokinins controls rice growth. *Plant Physiology*, **192**, 2457–2474.

Kim, D., **Langmead, B.** & **Salzberg, S.L.** (2015) HISAT: a fast spliced aligner with low memory requirements. *Nature Methods*, **12**, 357–360.

Kohlen, W., **Charnikhova, T.**, **Liu, Q.**, **Bours, R.**, **Domagalska, M.A.**, **Beguerie, S.** *et al.* (2011) Strigolactones are transported through the xylem and play a key role in shoot architectural response to phosphate deficiency in nonarbuscular mycorrhizal host Arabidopsis. *Plant Physiology*, **155**, 974–987.

Krasileva, K.V., **Vasquez-Gross, H.A.**, **Howell, T.**, **Bailey, P.**, **Paraiso, F.**, **Clissold, L.** *et al.* (2017) Uncovering hidden variation in polyploid wheat. *Proceedings of the National Academy of Sciences of the United States of America*, **114**, E913–E921.

Kurakawa, T., **Ueda, N.**, **Maekawa, M.**, **Kobayashi, K.**, **Kojima, M.**, **Nagato, Y.** *et al.* (2007) Direct control of shoot meristem activity by a cytokinin-activating enzyme. *Nature*, **445**, 652–655.

Liao, Y., **Smyth, G.K.** & **Shi, W.** (2014) FeatureCounts: an efficient general purpose program for assigning sequence reads to genomic features. *Bioinformatics*, **30**, 923–930.

Lorena Pantano. (2023) *DEGreport: report of DEG analysis*. Available at: https://bioconductor.org/packages/DEGreport [Accessed 12th April 2024].

Love, M.I., **Huber, W.** & **Anders, S.** (2014) Moderated estimation of fold change and dispersion for RNA-seq data with DESeq2. *Genome Biology*, **15**, 550.

Luo, L., **Pan, S.**, **Liu, X.**, **Wang, H.** & **Xu, G.** (2017) Nitrogen deficiency inhibits cell division-determined elongation, but not initiation, of rice tiller buds. *Israel Journal of Plant Sciences*, **64**, 32–40.

Machin, D.C., **Hamon-Josse, M.** & **Bennett, T.** (2020) Fellowship of the rings: a saga of strigolactones and other small signals. *New Phytologist*, **225**, 621–636.

Maeda, Y., **Konishi, M.**, **Kiba, T.**, **Sakuraba, Y.**, **Sawaki, N.**, **Kurai, T.** *et al.* (2018) A NIGT1-centred transcriptional cascade regulates nitrate signalling and incorporates phosphorus starvation signals in Arabidopsis. *Nature Communications*, **9**, 1376.

Martin, M. (2011) Cutadapt removes adapter sequences from high-throughput sequencing reads. *EMBnet J*, **17**, 10.

Marzec, M., **Situmorang, A.**, **Brewer, P.B.** & **Brąszewska, A.** (2020) Diverse roles of max1 homologues in rice. *Genes (Basel)*, **11**, 1–33.

Mashiguchi, K., **Sasaki, E.**, **Shimada, Y.**, **Nagae, M.**, **Ueno, K.**, **Nakano, T.** *et al.* (2009) Feedback-regulation of strigolactone biosynthetic genes and strigolactone-regulated genes in Arabidopsis. *Bioscience, Biotechnology, and Biochemistry*, **73**, 2460–2465.

Meng, X., **Wang, X.**, **Zhang, Z.**, **Xiong, S.**, **Wei, Y.**, **Guo, J.** *et al.* (2021) Transcriptomic, proteomic, and physiological studies reveal key players in wheat nitrogen use efficiency under both high and low nitrogen supply. *Journal of Experimental Botany*, **72**, 4435–4456.

Messing, S.A.J., **Mario Amzel, L.**, **Gabelli, S.B.**, **Echeverria, I.**, **Vogel, J.T.**, **Guan, J.C.** *et al.* (2010) Structural insights into maize viviparous14, a key enzyme in the biosynthesis of the phytohormone abscisic acid. *Plant Cell*, **22**, 2970–2980.

Minakuchi, K., **Kameoka, H.**, **Yasuno, N.**, **Umehara, M.**, **Luo, L.**, **Kobayashi, K.** *et al.* (2010) FINE CULM1 (FC1) works downstream of strigolactones to inhibit the outgrowth of axillary buds in rice. *Plant & Cell Physiology*, **51**, 1127–1135.

Müller, D., **Waldie, T.**, **Miyawaki, K.**, **To, J.P.C.**, **Melnyk, C.W.**, **Kieber, J.J.** *et al.* (2015) Cytokinin is required for escape but not release from auxin mediated apical dominance. *Plant Journal*, **82**, 874–886.

Raudvere, U., **Kolberg, L.**, **Kuzmin, I.**, **Arak, T.**, **Adler, P.**, **Peterson, H.** *et al.* (2019) G:profiler: a web server for functional enrichment analysis and conversions of gene lists (2019 update). *Nucleic Acids Research*, **47**, W191–W198.

Rubin, G., **Tohge, T.**, **Matsuda, F.**, **Saito, K.** & **Scheible, W.R.** (2009) Members of the LBD family of transcription factors repress anthocyanin synthesis and affect additional nitrogen responses in Arabidopsis. *Plant Cell*, **21**, 3567–3584.

Sakakibara, H. (2021) Cytokinin biosynthesis and transport for systemic nitrogen signaling. *Plant Journal*, **105**, 421–430.

Sakakibara, H., **Takei, K.** & **Hirose, N.** (2006) Interactions between nitrogen and cytokinin in the regulation of metabolism and development. *Trends in Plant Science*, **11**, 440–448.

Seale, M., **Bennett, T.** & **Leyser, O.** (2017) BRC1 expression regulates bud activation potential but is not necessary or sufficient for bud growth inhibition in Arabidopsis. *Development*, **144**, 1661–1673.

Seto, Y. (2024) Latest knowledge on strigolactone biosynthesis and perception. *Bioscience, Biotechnology, and Biochemistry*, **88**, 1–7.

Sigalas, P.P., **Buchner, P.**, **Thomas, S.G.**, **Jamois, F.**, **Arkoun, M.**, **Yvin, J.-C.** *et al.* (2023) Nutritional and tissue-specific regulation of cytochrome P450 CYP711A MAX1 homologues and strigolactone biosynthesis in wheat. *Journal of Experimental Botany*, **74**, 1890–1910. Available from: https://doi.org/10.1093/jxb/erad008

Soneson, C., **Love, M.I.** & **Robinson, M.D.** (2015) Differential analyses for RNA-seq: transcript-level estimates improve gene-level inferences. *F1000Res*, **4**, 1521.

Song, X., **Lu, Z.**, **Yu, H.**, **Shao, G.**, **Xiong, J.**, **Meng, X.** *et al.* (2017) IPA1 functions as a downstream transcription factor repressed by D53 in strigolactone signaling in rice. *Cell Research*, **27**, 1128–1141.

Soundappan, I., **Bennett, T.**, **Morffy, N.**, **Liang, Y.**, **Stanga, J.P.**, **Abbas, A.** *et al.* (2015) SMAX1-LIKE/D53 family members enable distinct MAX2-dependent responses to strigolactones and karrikins in Arabidopsis. *Plant Cell*, **27**, 3143–3159.

Sun, H., **Guo, X.**, **Qi, X.**, **Feng, F.**, **Xie, X.**, **Zhang, Y.** *et al.* (2021) SPL14/17 act downstream of strigolactone signalling to modulate rice root elongation in response to nitrate supply. *Plant Journal*, **106**, 649–660.

Sun, H., **Tao, J.**, **Liu, S.**, **Huang, S.**, **Chen, S.**, **Xie, X.** *et al.* (2014) Strigolactones are involved in phosphate- and nitrate-deficiency-induced root development and auxin transport in rice. *Journal of Experimental Botany*, **65**, 6735–6746.

Supek, F., **Bošnjak, M.**, **Škunca, N.** & **Šmuc, T.** (2011) Revigo summarizes and visualizes long lists of gene ontology terms. *PLoS One*, **6**, e21800.

Takei, K., **Ueda, N.**, **Aoki, K.**, **Kuromori, T.**, **Hirayama, T.**, **Shinozaki, K.** *et al.* (2004) AtIPT3 is a key determinant of nitrate-dependent cytokinin biosynthesis in Arabidopsis. *Plant Cell Physiology*, **45**, 1053–1062.

Takei, K., **Yamaya, T.** & **Sakakibara, H.** (2004) Arabidopsis CYP735A1 and CYP735A2 encode cytokinin hydroxylases that catalyse the biosynthesis of trans-zeatin. *Journal of Biological Chemistry*, **279**, 41866–41872.

Tarancón, C., **González-Grandío, E.**, **Oliveros, J.C.**, **Nicolas, M.** & **Cubas, P.** (2017) A conserved carbon starvation response underlies bud dormancy in woody and herbaceous species. *Frontiers in Plant Science*, **8**, 788.

The International Wheat Genome Sequencing Consortium. (2018) Shifting the limits in wheat research and breeding using a fully annotated reference genome. *Science*, **361**, eaar7191.

Uauy, C., **Wulff, B.B.H.** & **Dubcovsky, J.** (2017) Combining traditional mutagenesis with new high-throughput sequencing and genome editing to reveal hidden variation in polyploid wheat. *Annual Review of Genetics*, **51**, 435–454. Available from: https://doi.org/10.1146/annurev-genet-120116-

Ueda, Y., **Konishi, M.** & **Yanagisawa, S.** (2017) Molecular basis of the nitrogen response in plants. *Soil Science & Plant Nutrition*, **63**, 329–341.

Ueda, Y., **Ohtsuki, N.**, **Kadota, K.**, **Tezuka, A.**, **Nagano, A.J.**, **Kadowaki, T.** *et al.* (2020) Gene regulatory network and its constituent transcription factors that control nitrogen-deficiency responses in rice. *New Phytologist*, **227**, 1434–1452.

Umehara, M., **Hanada, A.**, **Magome, H.**, **Takeda-Kamiya, N.** & **Yamaguchi, S.** (2010) Contribution of strigolactones to the inhibition of tiller bud outgrowth under phosphate deficiency in rice. *Plant & Cell Physiology*, **51**, 1118–1126.

Umehara, M., **Hanada, A.**, **Yoshida, S.**, **Akiyama, K.**, **Arite, T.**, **Takeda-Kamiya, N.** *et al.* (2008) Inhibition of shoot branching by new terpenoid plant hormones. *Nature*, **455**, 195–200.

van Es, S.W., **Muñoz-Gasca, A.**, **Romero-Campero, F.J.**, **González-Grandío, E.**, **de Los Reyes, P.** *et al.* (2024) A gene regulatory network critical for axillary bud dormancy directly controlled by Arabidopsis BRANCHED1. *New Phytologist*, **241**, 1193–1209.

Wakabayashi, T., **Yasuhara, R.**, **Miura, K.**, **Takikawa, H.**, **Mizutani, M.** & **Sugimoto, Y.** (2021) Specific methylation of (11R)-carlactonoic acid by an Arabidopsis SABATH methyltransferase. *Planta*, **254**, 88.

Walker, C.H. & **Bennett, T.** (2018) Forbidden fruit: dominance relationships and the control of shoot architecture. *Annual Plant Reviews Online*, **1**, 217–254. Available from: https://doi.org/10.1002/9781119312994.apr0640

Wang, J., **Song, K.**, **Sun, L.**, **Qin, Q.**, **Sun, Y.**, **Pan, J.** *et al.* (2019) Morphological and transcriptome analysis of wheat seedlings response to low nitrogen stress. *Plants*, **8**, 98.

Wang, L., **Wang, B.**, **Jiang, L.**, **Liu, X.**, **Li, X.**, **Lu, Z.** *et al.* (2015) Strigolactone signaling in Arabidopsis regulates shoot development by targeting D53-like SMXL repressor proteins for ubiquitination and degradation. *Plant Cell*, **27**, 3128–3142.

Waters, M.T., **Brewer, P.B.**, **Bussell, J.D.**, **Smith, S.M.** & **Beveridge, C.A.** (2012) The Arabidopsis ortholog of rice DWARF27 acts upstream of MAX1 in the control of plant development by strigolactones. *Plant Physiology*, **159**, 1073–1085.

Waters, M.T., **Gutjahr, C.**, **Bennett, T.** & **Nelson, D.C.** (2017) Strigolactone signaling and evolution. *Annual Review of Plant Biology*, **68**, 291–322. Available from: https://doi.org/10.1146/annurev-arplant-042916-

Wheeldon, C.D. & **Bennett, T.** (2021) There and back again: an evolutionary perspective on long-distance coordination of plant growth and development. *Seminars in Cell & Developmental Biology*, **109**, 55–67.

Wu, S. & **Li, Y.** (2021) A unique sulfotransferase-involving strigolactone biosynthetic route in sorghum. *Frontiers in Plant Science*, **12**, 793459.

Xu, J., **Zha, M.**, **Li, Y.**, **Ding, Y.**, **Chen, L.**, **Ding, C.** *et al.* (2015) The interaction between nitrogen availability and auxin, cytokinin, and strigolactone in the control of shoot branching in rice (*Oryza sativa* L.). *Plant Cell Reports*, **34**, 1647–1662.

Yoneyama, K. & **Brewer, P.B.** (2021) Strigolactones, how are they synthesized to regulate plant growth and development? *Current Opinion in Plant Biology*, **63**, 102072.

Yoneyama, K., **Kisugi, T.**, **Xie, X.**, **Arakawa, R.**, **Ezawa, T.**, **Nomura, T.** *et al.* (2015) Shoot-derived signals other than auxin are involved in systemic regulation of strigolactone production in roots. *Planta*, **241**, 687–698.

Yoneyama, K., **Xie, X.**, **Kim, H.I.**, **Kisugi, T.**, **Nomura, T.**, **Sekimoto, H.** *et al.* (2012) How do nitrogen and phosphorus deficiencies affect strigolactone production and exudation? *Planta*, **235**, 1197–1207.

Yoneyama, K., **Xie, X.**, **Kusumoto, D.**, **Sekimoto, H.**, **Sugimoto, Y.**, **Takeuchi, Y.** *et al.* (2007) Nitrogen deficiency as well as phosphorus deficiency in sorghum promotes the production and exudation of 5-deoxystrigol, the host recognition signal for arbuscular mycorrhizal fungi and root parasites. *Planta*, **227**, 125–132.

Yoneyama, K., **Xie, X.**, **Nomura, T.** & **Yoneyama, K.** (2020) Do phosphate and cytokinin interact to regulate strigolactone biosynthesis or act independently? *Frontiers in Plant Science*, **11**, 438.

Yoneyama, K., **Xie, X.**, **Yoneyama, K.**, **Kisugi, T.**, **Nomura, T.**, **Nakatani, Y.** *et al.* (2018) Which are the major players, canonical or non-canonical strigolactones? *Journal of Experimental Botany*, **69**, 2231–2239.

Yoneyama, K., **Yoneyama, K.**, **Takeuchi, Y.** & **Sekimoto, H.** (2007) Phosphorus deficiency in red clover promotes exudation of orobanchol, the signal for mycorrhizal symbionts and germination stimulant for root parasites. *Planta*, **225**, 1031–1038.

Zha, M., **Zhao, Y.**, **Wang, Y.**, **Chen, B.** & **Tan, Z.** (2022) Strigolactones and cytokinin interaction in buds in the control of rice tillering. *Frontiers in Plant Science*, **13**, 837136.

Zhang, S., **Li, G.**, **Fang, J.**, **Chen, W.**, **Jiang, H.**, **Zou, J.** *et al.* (2010) The interactions among DWARF10, auxin and cytokinin underlie lateral bud outgrowth in rice. *Journal of Integrative Plant Biology*, **52**, 626–638.

Zhang, Y., **van Dijk, A.D.**, **Scaffidi, A.**, **Flematti, G.R.**, **Hofmann, M.**, **Charnikhova, T.** *et al.* (2014) Rice cytochrome P450 MAX1 homologs catalyze distinct steps in strigolactone biosynthesis. *Nature Chemical Biology*, **10**, 1028–1033.

Zhao, B., **Wu, T.T.**, **Ma, S.S.**, **Jiang, D.J.**, **Bie, X.M.**, **Sui, N.** *et al.* (2020) TaD27-B gene controls the tiller number in hexaploid wheat. *Plant Biotechnology Journal*, **18**, 513–525.